Thesis for the Degree of Licentiate of Engineering

A Compartmental Model for Kinetics of Apolipoprotein B-100 and Triglycerides in $VLDL_1$ and $VLDL_2$ in Normolipidemic Subjects

Martin Adiels

Department of Mathematics
Chalmers University of Technology
SE-412 96 Göteborg, Sweden
Göteborg, 2002

A Compartmental Model for Kinetics of Apolipoprotein B-100
and Triglycerides in $VLDL_1$ and $VLDL_2$ in Normolipidemic Subjects
MARTIN ADIELS

ISSN 0347-2809/NO 2002-11
Department of Mathematics
Chalmers University of Technology and Göteborg University
SE-412 96 Göteborg
Sweden
Telephone +46 (0)31-772 1000

This is a thesis of the ECMI (European Consortium for Mathematics in Industry) post-graduate program in Industrial Mathematics at Chalmers University of Technology.

The work was supported by the Wallenberg laboratory for cardiovascular research at The Sahlgrenska Academy at Göteborg University.

Matematiskt centrum
Göteborg, Sweden 2002

Abstract

Tracer/tracee experiments are commonly used in biochemistry. In this thesis we have applied the method to the kinetics of lipoproteins and their lipids. A short introduction to lipoproteins is given, and the theory of multi compartmental modelling and tracer/tracee kinetics are presented.
A compartmental model for the kinetics of apolipoprotein B-100 (apoB) and triglycerides (TG) is presented and applied to nine normolipidemic subjects, and one IGT subject. For the implementation of the model a commercial program called SAAMII was used. The fractional catabolic rate, fractional transfer rate, production and the delay time for apoB and TG were calculated. The production was 32 ± 14.5 grams of TG per day and 860 ± 290 mg of apoB per day. $92 \pm 3\%$ of the TG and $80 \pm 4\%$ of the apoB were secreted into the VLDL_1 subfraction. For the TG the delay time was 0.30 ± 0.07 hours and for apoB 0.52 ± 0.08 hours.
The aim of this thesis is to describe the mathematical model and the results.
We end the thesis by presenting how the project will be continued.

Keywords: Compartmental modelling, lipoprotein, apolipoprotein B, glycerol, triglycerides, tracer kinetics, stable isotope.

Preface

The thesis

This licentiate thesis is the mathematical result in an ongoing project in kinetics of lipoproteins and lipids. The project is a collaboration between Chalmers University of Technology, the Wallenberg laboratory for cardiovascular research at The Sahlgrenska Academy at Göteborg University and the Medical Department of Helsinki University.
The thesis is also the final result of the five semester ECMI program. ECMI stands for European Consortium For Mathematics in Industry and is a collaboration between universities in Europe for a program in applied mathematics. The first two semesters of the program consists of core courses and the next two semesters are individual courses focusing on the upcoming project. The last semester is devoted to a mathematical project originating from the industry.
This work was funded by NTM, Chalmers University of Technology and the Wallenberg laboratory.

Acknowledgements

I would like to thank my supervisor Assoc. Professor Bernt Wennberg. For having me in mind when this project first was presented, and for being encouraging and supporting. He has always been available for a chat and have read, and made comments to, this manuscript numerous times.
My medical supervisors Assoc. Professor Jan Borén, director of the Wallenberg laboratory and Professor Marja-Riitta Taskinen, University of Helsinki, have not only financially supported this project but have also been very helpful in questions concerning lipoproteins. I want to thank them for the help so far, and I am looking forward to the continuation of the project. After this mathematical thesis is written we will continue with the biological aspects of the results.
During the last year I have spent 3 months at the Royal Infirmary Hospital in Glasgow. I wish to express my gratitude to Dr Muriel Caslake and to all my friends there for making my stay pleasant, I am looking forward on going back. I specially wish to thank Professor Chris Packard for his comments on the model and his valuable thoughts on this project.
I would also like to thank all my friends at the Department of Mathematics, especially my fellow ECMI students Erik Alapää, Greger Cronquist, Henrik Olsson and Sara Ågren. They have made my years here easier and they are great friends. Random thanks goes to Robert Bohlin for across the corridor chats, Ola Helenius for windsurfing chats and Tobias, Erik, Anna, Fredik et al. for lunch chats. I also like to thank my supervisor for my master thesis,

Bo Johansson, for introducing me to ECMI.
Last but not least, I would like to thank my family. They have always supported me in my studies. Most of all, my thanks goes to Jenny for being there for me for the last 4 years, I could not have done this without her support.

Contents

List of common abbreviations

TG	triglyceride
Chyl	chylomicrons
HDL	high density lipoprotein
apoB	apolipoprotein B-100
apoB-100	apolipoprotein B-100
apoB-48	apolipoprotein B-48
VLDL	very low density lipoproteins
IDL	intermediate density lipoproteins
LDL	low density lipoproteins
LPL	lipoprotein *lipase*
(VL-I-L)DL	VLDL, IDL and LDL
HTGL	hepatic triglyceride lipase
IGT	impaired glucose tolerance

Some biomedicine terms

- triglyceride or triacylglycerol. An ester formed by glycerol and three (identical or different) fatty acids.
- phospholipids. A lipid containing one or more phosphate groups. Phospholipids are soluble in both water and lipids (amphipathic).
- lipase. Enzyme that catalyse the hydrolysis of triglyceride.
- hydrolysis. Reaction where water is added to produce two or more products.
- endocytosis. Uptake of extracellular material through the plasma membrane.

Introduction

Lipids, such as triglycerides and cholesterol, are transported in the blood by particles called lipoproteins. Particles that are rich in lipids have low density, but the density increase as the particles deliver their fat. The particles are classified according to their density. Here the very low density lipoprotein subclasses $VLDL_1$ and $VLDL_2$ are considered.
The aim of this thesis is to present a mathematical model that describes the kinetics of lipoproteins and triglycerides in the $VLDL_1$ and $VLDL_2$ subfractions. First an introduction to lipoproteins and especially to $VLDL_1$ and $VLDL_2$ metabolism is given. The theory of multi compartmental modelling, and tracer kinetics is shortly presented.
The kinetics of the particles are measured by measuring the kinetics of a protein molecule, called apolipoprotein B (apoB), attached to the particle. A compartmental model where apoB and TG are coupled is presented and applied to nine normolipidemic subjects and one IGT subject. The project is an ongoing work to develop a model that is applicable to normolipidemics, IGTs and subjects with type-2 diabetes. A time dependent model for a study where the subjects are given a constant injection of insulin will also be developed in the continuation of the project. This will give good statistical material to analyse the effects of insulin on secretion and composition of $VLDL_1$ and $VLDL_2$ particles.
Compartmental models have been used to model apoB (for instance [6], [8], [9] and [10]) and TG [16]. But they have never been modelled simultaneously before. The fundamental base of the model is an apoB model used in several studies, among others [6], [8], [9] and [10]. The possible applications of the model are abundant, not only in studies on diabetes but also in sports science and nutrition.
The author want to point out that his work at this point is mainly to derive the model, not to draw conclusions about the underlying biochemistry.
The study of lipoproteins and cholesterol is of great importance to research concerning coronary heart diseases and type-2 diabetes. Type-2 diabetes is a common disease in our society today, and the number of people suffering from this is increasing rapidly. Changes in lipoprotein metabolism are one of the early symptoms. The project is done in collaboration with Assoc. Professor Jan Borén, director of the Wallenberg laboratory for cardiovascular research at The Sahlgrenska Academy at Göteborg University and Professor Marja-Riitta Taskinen at the Department for Medicine, University of Helsinki. The data was collected and analysed in Helsinki and the enrichments were analysed in the Royal Infirmary University Hospital in Glasgow.

Chapter 1

Lipoproteins and their metabolism

Here is a short introduction to lipoproteins. It is not an attempt to fully describe the lipoprotein metabolism, but contains the most essential information needed to model the kinetics of lipoproteins and triglycerides. For further reading for instance [14] or [15] are recommended.
Lipids are not soluble in water, because they are hydrophobic. The particles transporting lipids and cholesterol in the blood are called lipoproteins. The core of the lipoproteins consists of *triglycerides* (TG) and cholesterol-esters. The shell is a mono-layer of amphipathic *phospholipids*. On the surface, proteins called apolipoproteins (see figure 1.1) are attached, which give the lipoproteins different characteristics. Lipoproteins are classified, depending on their different apolipoprotein content and on their density. Smaller particles have smaller TG content and therefore have higher density because lipids have lower density than pro-

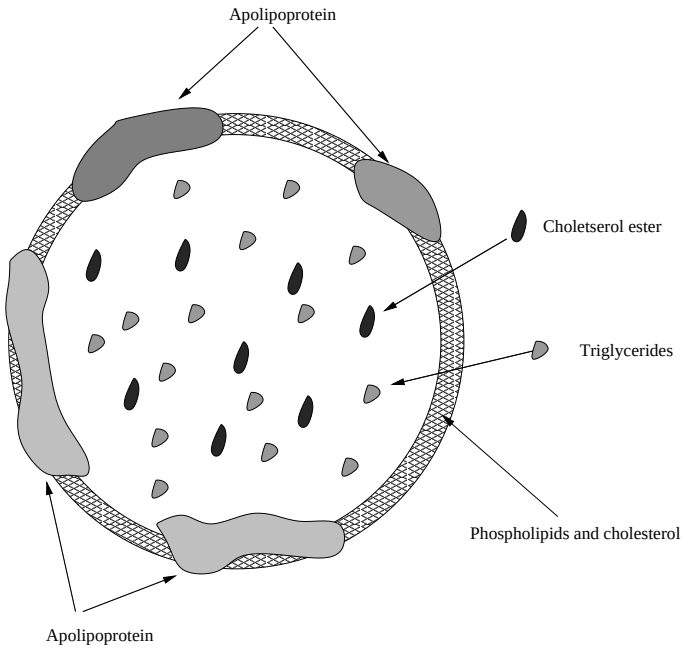

Figure 1.1: Structure of lipoproteins

teins.
The largest, and most TG-rich particles are called chylomicrons (Chyl). They are synthesised in the small-intestine and have a short residence time of about 30 minutes in the blood. Two types of lipoproteins are synthesised in the liver. High density lipoproteins (HDL) and the lipoproteins containing apoB-100. These apoB-100 containing lipoproteins are further divided into very low, intermediate and low density lipoproteins (VLDL, IDL and LDL) according to their density.
The three main types of lipoproteins differ not only in size and density, but also in their metabolism. The metabolism is governed by the different apolipoproteins attached to the particle. Chylomicrons have one molecule of apolipoprotein B-48 (apoB-48), while VLDL, IDL and LDL have one molecule of apoB-100, giving the (VL-I-L)DL and chylomicrons different metabolism. The apoB-48 and apoB-100 are identical up to the first 48% of the amino-acids. The apoB-100 molecule consists of 4536 amino acids, and is one of the largest protein-structures in humans. Some of the other apolipoproteins can be transferred between lipoproteins. For instance apoC can be transferred between HDL and VLDL.
This paper focus on VLDL metabolism and if nothing else is mentioned lipoproteins means the VLDL, IDL and LDL and apoB means apoB-100. To get a better discrimination between particles the VLDL fraction is further subdivided into $VLDL_1$ and $VLDL_2$, having $VLDL_1$ ranging from 400 to 60 Sf and $VLDL_2$ from 60 to 20 Sf. Sf, Svedberg flotation unit, is a measure of the rotational velocity needed to make a particle float, this is proportional to the density. It has been shown [10], [6] that there are metabolic differences between $VLDL_1$ and $VLDL_2$.
It should be pointed out that there is a continuous spectrum of densities within each subfraction of lipoproteins.

	Chyl	VLDL	IDL	LDL	HDL
density g/ml	<0.95	0.95-1.006	1.006-1.019	1.019-1.063	1.063-1.21
density S_f		20-400	12-20	0-12	
diameter nm	80-100	30-80	25-30	20-25	8-13
TG content %	90-95	50-65	25-40	4-6	7
CE %	2-4	8-14	20-35	34-35	10-20
FC %	1	4-7	7-11	6-15	5
PL %	2-6	12-16	16-24	22-26	25
protein %	1-2	5-10	12-16	22-26	45
major proteins	A-I (31)	C (40-50)	B-100 (60-80)	B-100 (>95)	A-I (65)
% of total	C (32)	B-100(30-40)	C (10-20)	C (<1)	A-II (10-23)
protein	E (10)	E (10-15)	E (10-15)	E (<1)	C (5-15)
	B-48 (5-8)				E (1-3)

Table 1.1: The different lipoproteins and their typical compositions. CE, cholesterol ester; FC, free cholesterol; PL, phospholipid.

1.1 Secretion of lipoproteins

VLDL particles are synthesised in the liver. Viewed in the perspective of apoB, first one molecule of apoB is synthesised and after that TG is added until the particle is big enough. A small fraction of these particles are secreted from the liver into the IDL and LDL subfractions. Once in the bloodstream, the lipoprotein gradually looses its TG content and becomes an IDL particle. Ultimately the particle becomes an LDL particle.

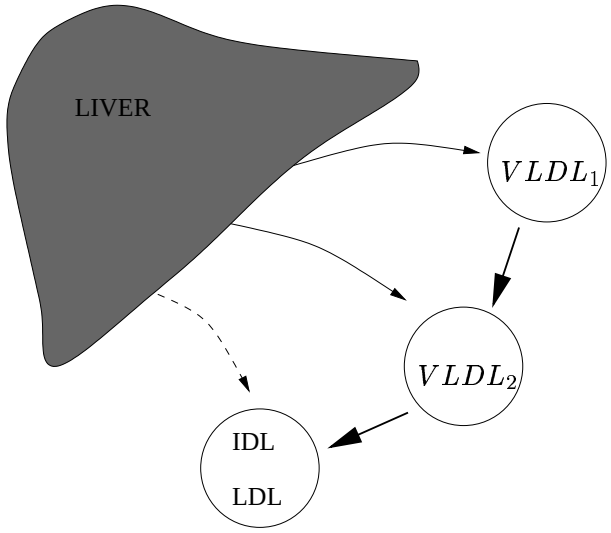

Figure 1.2: Most of the apoB containing lipoproteins are secreted in the $VLDL_1$ and $VLDL_2$ subfractions.

1.2 Lipoprotein metabolism

VLDL particles contain one apoB molecule but also apolipoprotein C and E (apoC and apoE). VLDL particles lose their TG content as the apoC activates the LPL in the capillaries of the peripheral tissues. As the *hydrolysis* continues, the density increases and the particle becomes an IDL particle. IDL particles have two fates. Either they may undergo further hydrolysis under the action of HTGL, loose their apoC and apoE to HDL and produce a cholesterol-rich LDL particle. Or, the IDL might be catabolised by *endocytosis* as the apoB and apoE allow the particles to bind to LDL-receptors. This is not possible for the larger VLDL particles, probably because of the larger size. Figure 1.2 shows a schematic view of lipoprotein metabolism. The LDL are rich in cholesterol and are commonly known as ”bad cholesterol” (i.e. atherogenic lipoproteins). The HDL is the ”good cholesterol”. The LDL particles can be further subdivided, in terms of density, into LDL I, II and III. These are in two pools LDL-α and LDL-β, which arise from different sources. Particles secreted into $VLDL_1$ becomes an LDL-β particle and the LDL-α particles arise from particles secreted into the $VLDL_2$, IDL and LDL subfractions, as shown in figure 1.4. The LDL particles contain no or very little apoC and apoE.

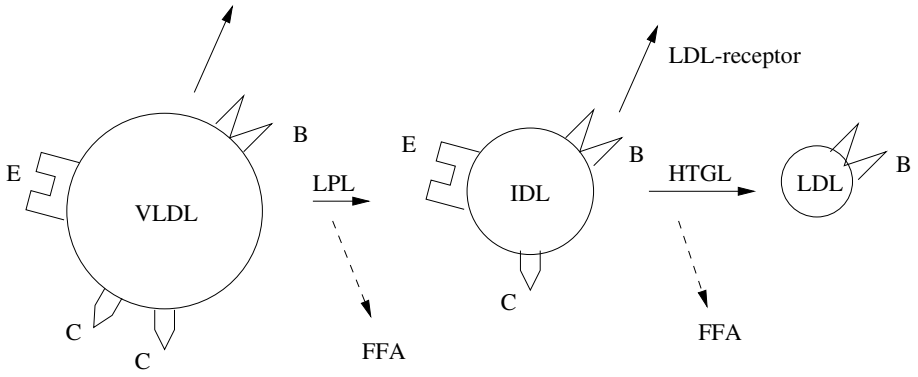

Figure 1.3: Schematic view of lipoprotein metabolism

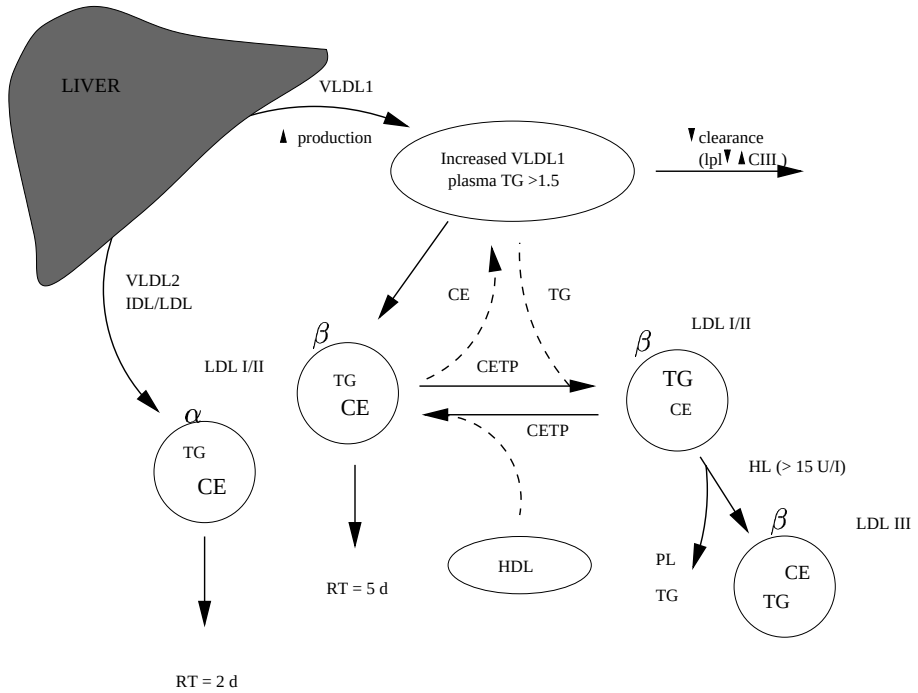

Figure 1.4: Kinetic evidence suggests that the two metabolically distinct pools in LDL (α and β) arise from different sources. Pool α is the major species detected in subjects with low to normal plasma triglyceride (TG) levels. LDL with the kinetic properties of pool β result from delipidation of $VLDL_1$. The two LDL species have substantially different residence times (RT) in the circulation. LDL-III generation is favored when the plasma triglyceride level is > 1.5 mmol/l. As plasma triglyceride levels rise, $VLDL_1$ accumulate because of overproduction or defective removal. The action of HL removes lipid from the LDL-II to form LDL-III. CE, cholesterol ester; CETP, cholesterol ester transfer protein; PL, phospholipids.

1.2.1 $VLDL_1$ and $VLDL_2$ metabolism

All particles in the $VLDL_1$ fraction come directly from the liver. A $VLDL_1$ particle can either be converted to $VLDL_2$ under the action of LPL or it can be consumed by catabolism. The $VLDL_2$ particles come from two sources, the $VLDL_1$ and the liver. The different metabolisms of $VLDL_2$ secreted from the liver and $VLDL_2$ derived from $VLDL_1$ [10], [6] suggest that there are two different pathways for $VLDL_2$, as shown in figure 1.5. The residence time for $VLDL_1$ is 1-4 hours and for $VLDL_2$ 3-7 hours.
When modelling the metabolism it is assumed that particles have fixed densities or sizes, e.g. a particle can only have a fixed number of different densities. It is important to keep in mind that there is a continuous spectrum of densities, and that hydrolysis is a process that slowly decrease the TG content. The number of possible density classes could of course be increased, which may be more accurate since the particle density spectrum is not discrete. VLDL could be divided in three or four groups instead of two. Under the same assumption that the initial particle size affects its kinetics a model as in figure 1.6 could be considered.
The model that have been developed are somewhere in between these two examples. There is a question of how well things can be measured in order to adjust the unknown parameters. To get accurate measurements a certain amount of blood is needed for each fraction and hence a large quantity of blood is needed to get many fractions. The complexity of the model is therefore limited by the number of fractions that can be measured.
The primary goal was to develop a $VLDL_1$ and $VLDL_2$ model for apoB and TG in normal subjects. The main difference in metabolism of $VLDL_2$ secreted direct from liver and $VLDL_2$ derived from $VLDL_1$ becomes most apparent in the LDL subfraction. Therefore only one pathway for $VLDL_2$ particles are needed to model $VLDL_1$ and $VLDL_2$.

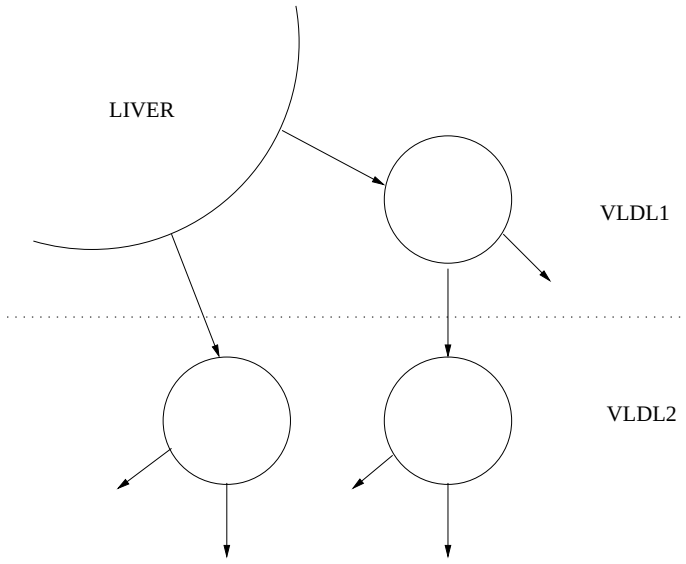

Figure 1.5: Schematic view of $VLDL_1$ and $VLDL_2$ metabolism

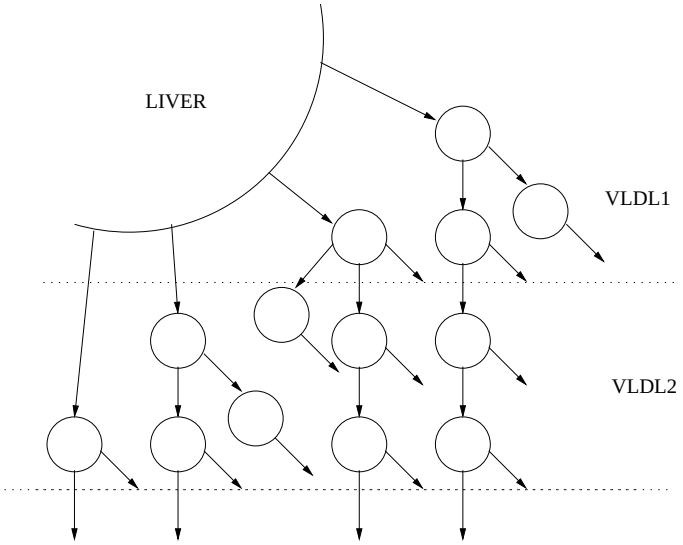

Figure 1.6: Schematic view of suggested 4-level VLDL metabolism. Catabolism of newly secreted particles are not direct but via a remnant group of particles from which they are removed.

Chapter 2

Multi compartmental modelling

When modelling biological, chemical and physiological experiments ordinary and/or partial differential equations (ODE, PDE) are often used to describe the experiment. For instance one can describe the kinetic of lipoprotein particles by an ODE system. Let $b(t)$ be the number of apoB molecules in the liver, and $v(t)$, $i(t)$ and $l(t)$ be number of apoB molecules in VLDL, IDL and LDL respectively. The input of new particles into the liver is $u(t)$ (as described later, this liver model is an oversimplification). The transfer rates of particles between liver and VLDL, VLDL and IDL and IDL and LDL are denoted $T_{v,b}$, $T_{i,v}$ and $T_{l,i}$. There may also be losses by direct catabolism of particles; denote these by C_α where $\alpha = b, v, i, j$. The equations describing the change of number of particles are

$$\begin{cases} \frac{db}{dt} &= u(t) - T_{v,b}(b,v,t) - C_b(b,t), \\ \frac{dv}{dt} &= T_{v,b}(b,v,t) - T_{i,v}(v,i,t) - C_v(v,t), \\ \frac{di}{dt} &= T_{i,v}(v,i,t) - T_{l,i}(i,l,t) - C_i(i,t), \\ \frac{dl}{dt} &= T_{l,i}(i,l,t) - C_l(l,t). \end{cases}$$

A way to obtain these equations is *multi compartmental modelling*. Multi compartmental modelling is commonly used in biochemistry and [11] is recommended for further reading. For a more mathematical description [1] or chapter 8 in [12] gives a good introduction. The following definitions can be found in [1] or [12].

Definition 1 (Compartment). A compartment is a well-mixed and kinetically homogeneous amount of material. A multi compartmental system is a finite set of compartments that interact by exchanging material. A multi compartment model is the mathematical equations describing the fluxes of material.

A compartment does not necessary correspond to a physical volume. In a chemical reaction with substance A and B, $A + B \rightleftharpoons AB$ one compartment may represent free mass of A and one compartment the mass of A bound to AB.

Definition 2 (Fractional transfer coefficient). The fraction of material transferred from compartment i to compartment j per time unit is called the fractional transfer coefficient and is denoted $k(j,i)$ or $k_{j,i}$. The flux from compartment i to compartment j is denoted $FLUX(j,i) = k(j,i)\ Q_i$, where Q_i is the mass in compartment i.

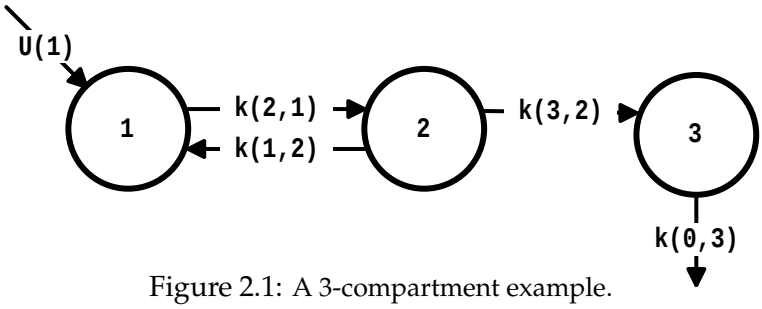

Figure 2.1: A 3-compartment example.

A compartmental model is often described graphically by circles or boxes (compartments) and arrows (fluxes) connecting the circles, as in figure 2.1. Throughout this thesis Q_i or q_i are used for the amount of material in a compartment i. Loss from a compartment i (not to other compartments) is described as a flux to the environment (or a compartment 0), and the corresponding fractional transfer coefficient is $k_{0,i}$. External input of material to compartment i is denoted $U_i(t)$. The equation for the rate of change of material in a compartment i in an n compartment system is

$$\frac{dQ_i(t)}{dt} = \sum_{\substack{j=1 \\ j\neq i}}^{n} k_{i,j}(\mathbf{Q},t)Q_j - \sum_{\substack{j=0 \\ j\neq i}}^{n} k_{j,i}(\mathbf{Q},t)Q_i + U_i(t). \tag{2.1}$$

Define $k_{i,i} = -\sum_{\substack{j=0 \\ j\neq i}}^{n} k_{j,i}(\mathbf{Q},t)$,

$$\frac{dQ_i(t)}{dt} = \sum_{j=1}^{n} k_{i,j}(\mathbf{Q},t)Q_j + U_i(t). \tag{2.2}$$

The resulting system can be formulated as

$$\frac{d\mathbf{Q}(t)}{dt} = \mathbf{K}(\mathbf{Q},t)\mathbf{Q}(t) + \mathbf{U}(t) \tag{2.3}$$

Definition 3 (Linear multi compartmental models). A multi compartmental model of n compartments is linear if all $k_{j,i}$ are constants or depend on time only.

For linear models (which are the most common) it is often useful to write the input $\mathbf{U}(t)$ as $\mathbf{B}\mathbf{V}(t)$, where $\mathbf{B}$ is an n by m matrix and $\mathbf{V} \in \mathbb{R}^m_+$. The reason is that the input to one compartment may be a linear combination of more than one input. An input may go to more than one compartment in an unknown proportion, but in most cases the matrix $\mathbf{B}$ consists of 0s and 1s. $\mathbf{B}$ is called the *input distribution matrix*.

Definition 4 (Steady-state). A multi compartmental model $\frac{d\mathbf{Q}(t)}{dt} = \mathbf{K}(\mathbf{Q},t)\mathbf{Q}(t) + \mathbf{U}(t)$ is in steady-state if the input $\mathbf{U}$ and $\mathbf{K}$ are independent of time, and the change of masses is 0.

The resulting equation in a steady-state model is

$$-\mathbf{U} = \mathbf{K}\mathbf{Q}. \tag{2.4}$$

In experiments samples are taken at compartments, or cluster of compartments. For obvious reasons it is not always possible to sample all compartments. The function that is sampled is $\mathbf{S}(t) = \mathbf{C}\mathbf{Q}(t)$. If the samples are taken at m places $\mathbf{S} \in \mathbb{R}^m$ and $\mathbf{C}$ is an m by n matrix. A more general definition can be made with the definition of an output.

Definition 5 (Output). An output is a linear combination of compartments connected to a recording device. The function $S(t) = \mathbf{c}^T\mathbf{Q}(t)$ is used to describe an output, $\mathbf{c}$ is a vector of size n. If there are m outputs these are numbered $S_i(t) = \mathbf{c}_i^T\mathbf{Q}(t),\ i = 1, \ldots, m$.

Note. $\mathbf{C} = [\mathbf{c}_1 \cdots \mathbf{c}_m]^T$, *but the latter definition is more general since the sampling of the outputs are not necessarily done at the same time points.*

The equations are

$$\begin{aligned} \frac{\mathbf{Q}(t)}{dt} &= \mathbf{K}(\mathbf{Q}, t)\mathbf{Q}(t) + \mathbf{B}\mathbf{V}(t) \\ S_i(t) &= \mathbf{c}_i^T\mathbf{Q}(t),\ i = 1, \ldots, m \end{aligned} \tag{2.5}$$

Both equation (2.3) and (2.5) are used to describe the system.

2.1 Properties of the systems

From equation (2.1) and (2.2) some properties of the system (2.3) can be formulated. For the matrix $\mathbf{K}$ the following holds

i) Every diagonal element is non-positive ($k_{i,i} \leq 0$).

ii) Every off diagonal element is non-negative ($k_{i,j} \geq 0,\ j \neq i$).

iii) The column sums are non-positive ($-k_{0,i} \leq 0$).

Definition 6 (Compartmental matrix). A matrix satisfying i)-iii) is called a compartmental matrix.

Definition 7 (Exit). A compartment i having $k_{0,i} > 0$ is called an exit.

Let E denote the set of exits. A (directed) graph of a n by n matrix $\mathbf{A}$ is a set of n nodes, connected by arrows. Two nodes i and j are connected with an arrow from i to j if $\mathbf{A}\ (i, j)\ \neq\ 0$.

Definition 8 (Reachable). A compartment j is reachable from a compartment i if the graph of $\mathbf{K}^T$ contains a path between i and j.

For a compartment i the set of reachable compartments can be defined as $R_i = \{j : i \text{ reaches } j\}$.

Definition 9 (Open). A compartmental system is called open if every compartment can reach an exit.

The condition for openness can also be formulated as $R_i \bigcap E \neq \emptyset, \forall i = 1, \ldots, n$, where $\emptyset$ denotes the empty set.
Gershgorins theorem states that each eigenvalue of a matrix $\mathbf{B}$ lies in the union of the n disks $|\lambda - b_{i,i}| \leq \sum_{\substack{j=1 \\ j\neq i}}^{n} |b_{i,j}|$. For the matrix $\mathbf{K}$ the centers of the disks are in $k_{i,i} \leq 0$ and the radius is less than or equal to $-k_{i,i}$. Hence the real part for each eigenvalue λ of $\mathbf{K}$ are non positive ($\Re(\lambda) \leq 0$) and no eigenvalue is purely imaginary.
In an open system with no external input (for $t > 0$) and with an initial amount of material in each compartment, the equation for the change of material is $\frac{d\mathbf{Q}(t)}{dt} = \mathbf{K}\mathbf{Q}(t)$. Clearly

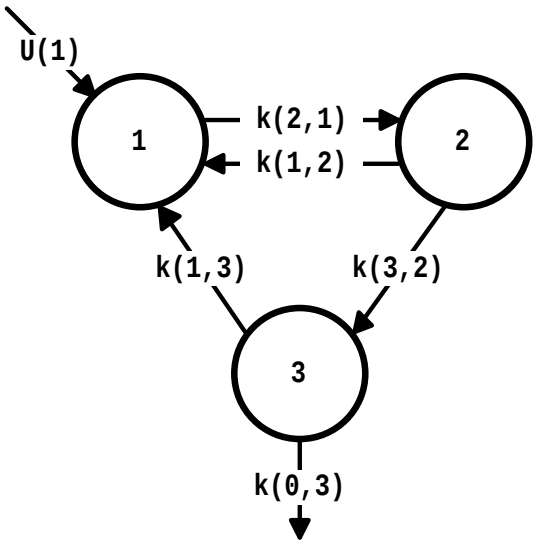

Figure 2.2: An example of a compartmental model with a circuit of length 3. The indices in the circuit are 3,1,2.

$\mathbf{Q}(t) \to 0$ as $t \to \infty$, and the system cannot have a constant particular solution i.e. no eigenvalue of $\mathbf{K}$ is 0. Hence $\Re(\lambda) < 0$ for every eigenvalue λ, and therefore $\mathbf{K}$ is nonsingular.
A *circuit* of a graph is a set of distinct indices $j_1, \dots\ j_K$ such that $k_{j_1,j_2}, \dots\ , k_{j_{K-1},j_K}, k_{j_K,j_1} \neq 0$, as in the example in figure 2.2. If λ is an eigenvalue of $\mathbf{K}$ then $\lambda + \alpha$ is an eigenvalue of $\mathbf{M} = \alpha\mathbf{I} + \mathbf{K}$, also if $\mathbf{K}$ is irreducible then $\mathbf{M}$ is irreducible. Theorem 1 in [7] states that if $\mathbf{M}$ is irreducible and non-negative and the longest circuit in the graph of $\mathbf{M}$ has length 2, then all eigenvalues of $\mathbf{M}$ are real.
If $\alpha \in \mathbb{R}$ is chosen such that $\mathbf{M} = \alpha\mathbf{I} + \mathbf{K} \geq 0$, $\mathbf{K}$ is irreducible and the longest circuit of $\mathbf{K}$ are of length 2 then all eigenvalues of $\mathbf{K}$ are real.

2.2 Tracer/tracee experiments

Consider an experiment to study the amount of lipoproteins secreted from the liver per hour. If the lipoproteins are characterised by their density, a particle newly secreted from the liver cannot be distinguished from a particle that have circulated the system for a while. Therefore it is impossible to describe the kinetics of the particles. This is a case where tracer/tracee experiments are useful. By introducing markers or labels on some of the particles secreted from the liver, these can be followed by measuring the concentration of labelled particles. The labelled material is called the tracer and the material being studied is called the tracee. Knowledge about the kinetics of the tracee can be gained by studying the kinetics of the tracer.
When choosing the tracer one must consider several aspects, the most important are

i) The biological system should not be able to distinguish between the tracee and the tracer.

ii) In steady-state experiments, the amount of tracer should be small enough not to affect

the steady-state.

iii) If the tracer is an isotope, there should be no exchange of isotope between labelled compounds and other compounds, and the natural occurrence of the isotope should be negligible or at least under control.

Let $\mathbf{Q}$ be the mass of the tracee and $\mathbf{q}$ the mass of the tracer. The system for the total mass is

$$\frac{d(\mathbf{Q}(t)+\mathbf{q}(t))}{dt} = \mathbf{K}(\mathbf{Q}+\mathbf{q}(t),t)(\mathbf{Q}(t)+\mathbf{q}(t))+\mathbf{U}(t)+\mathbf{u}(t),$$

where $\mathbf{u}(t)$ is the input of tracer. Or, for a single compartment

$$\frac{d(Q_i(t)+q_i(t))}{dt} = \sum_{j=1}^{n} k_{i,j}(\mathbf{Q}+\mathbf{q},t)(Q_j+q_j)+U_i(t)+u_i(t).$$

If the mass of the tracer is assumed to be small compared to the tracee mass, the right hand side can be Taylor expanded in $\mathbf{Q}$

$$\begin{aligned} &\approx \sum_{j=1}^{n} k_{i,j}(\mathbf{Q},t)Q_j+U_i(t)+ \\ &+\sum_{j=1}^{n}(\sum_{l=1}^{n}\frac{dk_{i,j}(\mathbf{Q},t)}{dQ_l}Q_j+k_{i,j}(\mathbf{Q},t))q_j+ \\ &+u_i(t)+O(\|q\|^2). \end{aligned}$$

Subtracting (2.2)

$$\begin{aligned} \frac{dq_i(t)}{dt} &\approx \sum_{j=1}^{n}(\sum_{l=1}^{n}\frac{dk_{i,j}(\mathbf{Q},t)}{dQ_l}Q_j+k_{i,j}(\mathbf{Q},t))q_j+ \\ &+u_i(t)+O(\|q\|^2). \end{aligned}$$

If the amount of tracer is small, the quadratic term can be neglected, and the resulting system is linear in $\mathbf{q}$

$$\frac{dq_i(t)}{dt} = \sum_{j=1}^{n}(\sum_{l=1}^{n}\frac{dk_{i,j}(\mathbf{Q},t)}{dQ_l}Q_j+k_{i,j}(\mathbf{Q},t))q_j+u_i(t).$$

In the linear case, the equations are

$$\frac{d(\mathbf{Q}(t)+\mathbf{q}(t))}{dt} = \mathbf{K}(t)(\mathbf{Q}(t)+\mathbf{q}(t))+\mathbf{U}(t)+\mathbf{u}(t),$$

subtracting (2.3)

$$\frac{d\mathbf{q}(t)}{dt} = \mathbf{K}(t)\mathbf{q}(t)+\mathbf{u}(t). \tag{2.6}$$

2.3 Sampling

In experiments the outputs are sampled. Let m be the number of outputs and N_i the number of time points when the i:th output is sampled, and $t_{i,j}$ the j:th time point, $j=1,\ldots,N_i$ and $i=1,\ldots,m$. The outputs are usually ordered so that the tracee outputs are $1,\ldots,m^e$ and the tracer outputs $m^e+1,\ldots,m$. The samples are denoted $\phi_{i,j}$ and if $\phi_{i,j}$ is a sample of $S_i(t_{i,j})$ we write $\phi_{i,j}\sim S_i(t_{i,j})$. Here $\phi_{i,j}\sim S_i(t_{i,j})=\mathbf{c}_i^T\mathbf{Q}(t_{i,j})$ for $i=1,\ldots,m^e$ and $\phi_{i,j}\sim S_i(t_{i,j})=\frac{\mathbf{c}_i^T\mathbf{q}(t_{i,j})}{\mathbf{c}_i^T\mathbf{Q}(ti,j)}$ for $i=m^e+1,\ldots,m$.

2.4 Modelling delays

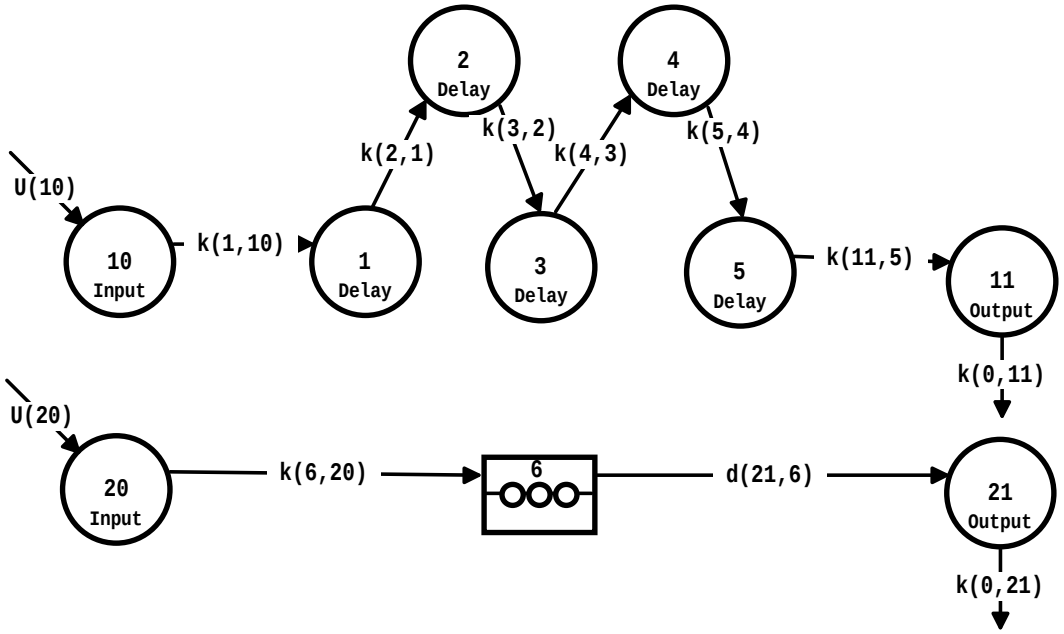

Figure 2.3: Delay as a compartmental system. The symbol for compartment 6 will be used for delays.

Reactions may not be instant, and therefore delays must be considered. There are several ways of implementing delays, here the method used by the SAAMII program (Section 2.8) is described. Consider an in-signal as in figure 2.4(a). A mathematical delay will, as shown in figure 2.4(b) give a time shift of the input function. But a more physiological delay might be a more blurred or diffuse delay, as in figure 2.4(c) and 2.4(d). The delay can be modelled as a number of compartments M with the same transfer-coefficients k_D. T_D is defined to be the time it takes for the first compartment after the delay to reach its maximum amount given an instant input to the delay. The equations are

$$\frac{d}{dt}\begin{pmatrix} Q_1 \\ Q_2 \\ \vdots \\ Q_n \end{pmatrix} = \begin{pmatrix} -k_D & 0 & 0 & 0 & 0 \\ k_D & -k_D & 0 & 0 & 0 \\ 0 & \ddots & \ddots & \ddots & 0 \\ 0 & \ddots & k_D & -k_D & 0 \\ 0 & 0 & 0 & k_D & -k_D \end{pmatrix} \begin{pmatrix} Q_1 \\ Q_2 \\ \vdots \\ Q_n \end{pmatrix} + \begin{pmatrix} f(t) \\ 0 \\ \vdots \\ 0 \end{pmatrix},$$

or

$$\frac{d\mathbf{Q}(t)}{dt} = \mathbf{K}\mathbf{Q}(t) + \mathbf{U}(t). \tag{2.7}$$

To decide how to choose k_D, fix n and use a instant input

$$\begin{aligned} \mathbf{U} &= \mathbf{0} \\ \mathbf{Q}_0 &= \begin{pmatrix} 1 & 0 & \cdots & 0 \end{pmatrix}^T, \end{aligned} \tag{2.8}$$

The solution to (2.7) - (2.8) is

$$\mathbf{Q}(t) = e^{Kt}\mathbf{Q}_0$$

Note that $\mathbf{K} = -k_D\mathbf{I} + k_D\mathbf{N}$, where $\mathbf{N}$ has ones on the first sub-diagonal. Clearly $\mathbf{IN} = \mathbf{NI}$, so

$$\begin{aligned} e^{\mathbf{K}t} &= e^{-k_D t\mathbf{I}} e^{k_D t\mathbf{N}} \\ &= e^{-k_D t}(\mathbf{I} + k_D t\mathbf{N} + \cdots + (k_D t)^{n-1}\frac{\mathbf{N}^{n-1}}{(n-1)!}). \end{aligned}$$

This gives an equation for the mass in the i:th compartment

$$Q_i(t) = e^{-k_D t}\frac{(k_D t)^{i-1}}{(i-1)!}.$$

The maximum is attained when $\dot{\mathbf{Q}} = 0$, i.e.

$$\begin{aligned} 0 = \frac{dQ_i}{dt} &= -k_D e^{-k_D t}\frac{(k_D t)^{i-1}}{(i-1)!} + e^{-k_D t}(i-1)\frac{(k_D t)^{i-2}}{(i-1)!} \\ &= e^{-k_D t}\frac{(k_D t)^{i-2}}{(i-1)!}k_D(-k_D t + (i-1)). \end{aligned}$$

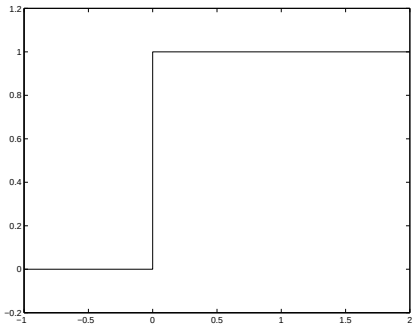

(a) in-signal

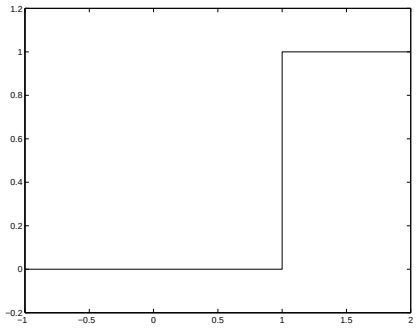

(b) time shifted signal

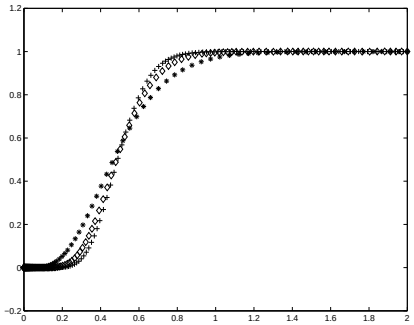

(c) delay-time 0.5 h

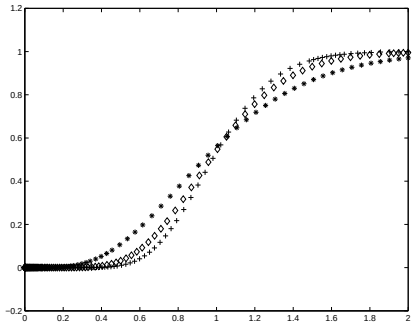

(d) delay-time 1 h

Figure 2.4: Delays modelled as in figure 2.3 for $T_D = 0.5$ and $T_D = 1$. Input signal is a constant function. 5 compartments - '$*$', 10 compartments - '$\diamond$' and 15 compartments - '$+$'. Notice that the sharpness of the delay depends on the number of compartments and the desired delay-time.

So compartment i in the delay attains its maximum at $t = (i-1)/k_D$, hence the first compartment after the delay attains its maximum at $t = n/k_D$. Therefore choose $k_D = n/T_D$.

2.5 Linear ODE

The systems that arise are of the form

$$\begin{aligned} \dot{\mathbf{Q}}(t) &= \mathbf{K}(t)\,\mathbf{Q}(t) + \mathbf{U}(t), \\ \mathbf{Q}(0) &= \mathbf{Q}_0. \end{aligned}$$

There is a very large literature on ODE-systems, and here only give a short introduction to linear equations is given. Consider a constant coefficient problem

$$\dot{\mathbf{Q}}(t) = \mathbf{K}\,\mathbf{Q}(t) + \mathbf{U}(t), \tag{2.9}$$

$$\mathbf{Q}(0) = \mathbf{Q}_0. \tag{2.10}$$

The homogeneous system $\dot{\mathbf{Q}}(t) = \mathbf{K}\,\mathbf{Q}(t)$ has the solution $\mathbf{Q}(t) = e^{\mathbf{K}\,t}\mathbf{c}$, for any $\mathbf{c} \in \mathbb{R}^n$. For a (square) matrix $\mathbf{A}$, $e^{\mathbf{A}}$ is defined as

$$e^{\mathbf{A}} = \mathbf{I} + \mathbf{A} + \frac{\mathbf{A}^2}{2!} + \frac{\mathbf{A}^3}{3!} + \cdots .$$

A particular solution to (2.9)-(2.10) is given by

$$\mathbf{Q}(t) = \int_0^t e^{\mathbf{K}(t-s)}\mathbf{U}(s)ds + e^{\mathbf{K}\,t}\mathbf{Q}_0.$$

The input function $\mathbf{U}(t)$ is often constant for the tracee and the tracer (in many cases the tracer is an instant injection and therefore $\mathbf{u}(t) = 0$). In these cases the solution is (if K is nonsingular)

$$\begin{aligned} \mathbf{Q}(t) &= [-e^{\mathbf{K}\,(t-s)}\mathbf{K}^{-1}\,\mathbf{U}]_{s=0}^{s=t} + e^{\mathbf{K}\,t}\mathbf{Q}_0 \\ &= e^{\mathbf{K}\,t}(K^{-1}\mathbf{U} + \mathbf{Q}_0) - \mathbf{K}^{-1}\,\mathbf{U}. \end{aligned}$$

A solution to the linear model, equation (2.6) with $\mathbf{u}(t) = 0$ can be written as

$$\mathbf{q}(t) = c_i \sum_{i=1}^{n} e^{\lambda_i t}\mathbf{v}_i.$$

Where c_i are constants, λ_i are eigenvalues of $\mathbf{K}$ and $\mathbf{v}_i$ the corresponding eigenvector. If the eigenvalues have negative real part, then the solution will be damped and go to 0 as t goes to grows. If the eigenvalues are real, then there cannot be any oscillations.

2.6 Optimisation - fitting curves

As for ODE's, there is an extensive literature on optimisation and the aim of this thesis is not to fully cover these theories.

In a general ODE model there are measurements Φ_i of a known function $\mathbf{Y}(t)$ at time points $t = t_i$,

$$(*)\begin{cases} \mathbf{Y}(t) &= \mathbf{G}(\mathbf{Q}, \mathbf{p}, t) \\ \dot{\mathbf{Q}}(t) &= \mathbf{F}(\mathbf{Q}, \mathbf{p}, t) \\ \mathbf{Q}(0) &= 0 \end{cases}$$

where $\mathbf{p}$ is the set of unknown parameters.

Note. $\mathbf{G}$ *can depend on* $\mathbf{p}$ *since an unknown proportion of compartments might be measured. Initial amounts can be treated as instant injections and* $\mathbf{Q}(0) = \mathbf{0}$.

The problem is to find

$$\min_{\mathbf{p}} \sum_{i=1}^{n} \text{error}(\Phi_i, \mathbf{Y}(\mathbf{p}, t_i))$$

subject to $(*)$, where $\mathbf{Y}(t) = \mathbf{Y}(\mathbf{p}, t)$ and $\text{error}(\Phi_i, \mathbf{Y}(\mathbf{p}, t_i))$ is a measure of the error between the calculated and measured value at the i:th time point. In the linear tracer/tracee compartmental case the samples are as in Section 2.3. The objective function is defined as

$$\mathrm{O}(\mathbf{p}) \quad = \quad \sum_{i=1}^{m} \sum_{j=1}^{N_i} \text{error}(\phi_{i,j}, S_i(\mathbf{p}, t_{i,j})).$$

The minimising problem is,

$$\min_{\mathbf{p}} \mathrm{O}(\mathbf{p}),$$

subject to S_i being solutions to the system

$$(**)\begin{cases} S_i(\mathbf{p}, t_{i,j}) &= \mathbf{c}_i^T \mathbf{Q}(t_{i,j}),\ i = 1, \ldots, m^e \\ S_i(\mathbf{p}, t_{i,j}) &= \frac{\mathbf{c}_i^T \mathbf{q}(t_{i,j})}{\mathbf{c}_i^T \mathbf{Q}(t_{i,j})}, i = m^e + 1, \ldots, m, \\ \dot{\mathbf{Q}}(t) &= \mathbf{K}(\mathbf{p}, t)\ \mathbf{Q} + \mathbf{U}(\mathbf{p}, t) \\ \dot{\mathbf{q}}(t) &= \mathbf{K}(\mathbf{p}, t)\ \mathbf{q} + \mathbf{u}(\mathbf{p}, t) \\ \mathbf{Q}(0) &= \mathbf{Q}_0(p) \\ \mathbf{q}(0) &= \mathbf{q}_0(p) \end{cases} .$$

Note. $\mathbf{q}_0$ *is usually known, but it might be the case that one injection goes into more than one compartment and in an unknown proportion.*

How should the error function $\text{error}(\tilde{\mathbf{x}}, \mathbf{x})$ be chosen?

2.6.1 Least squares

A possible approach could be to define $\text{error}(\tilde{\mathbf{x}}, \mathbf{x}) = \sum_i |\tilde{x}_i - x_i|$ i.e. the distance between the components in $\tilde{\mathbf{x}}$ and $\mathbf{x}$, and the total distance between the measured and calculated values are minimised. But this function has some drawbacks; it is not differentiable and the penalty for large errors is too small. For example; every point between two points (say 0 and 10)

have the same total distance to them. Given three points 0, 0 and 10, the point 0 has the smallest total distance to the three points. Clearly the distance is not a good error function. The function $\text{error}(\tilde{\mathbf{x}}, \mathbf{x}) = \sum_i (\tilde{x}_i - x_i)^2$ is differentiable and have a quadratic penalty. This gives the least squares estimation and is the most common curve fitting method. In the two examples above, the points 5 and 3.333 are the best approximations. The least squares objective function is

$$\mathrm{O_{LS}}(\mathbf{p}) = \sum_{i=1}^{m}\sum_{j=1}^{N_i}(\phi_{i,j} - S_i(\mathbf{p}, t_{i,j}))^2.$$

Assume that $\mathbf{K}(\mathbf{p}, t)$ and $\mathbf{U}(\mathbf{p}, t)$ are the correct model. Then there exists an parameter vector $\bar{\mathbf{p}}$ such that

$$\phi_{i,j} = S_i(\bar{\mathbf{p}}, t_{i,j}),$$

and hence

$$\mathrm{O_{LS}}(\bar{\mathbf{p}}) = 0,$$

where $\bar{\mathbf{Q}}$ solves

$$\dot{\mathbf{Q}}(t) = \mathbf{K}(\bar{\mathbf{p}}, t)\ \mathbf{Q} + \mathbf{U}(\bar{\mathbf{p}}, t).$$

Least squares is a very common technique in parameter estimation, numerical analysis and optimisation. The reasoning above is an attempt to explain least squares to non-mathematicians. There are a great literature in least squares and it can be found in almost any book in numerical analysis, statistics, optimisation etc. For the implementation used here, books like [5] and [12] on Regression Analysis or [4] on nonlinear parameter estimation are recommended for further reading.

A more mathematical justification for least squares is that if the errors are independent and identically distributed $\mathrm{N}(0, \sigma^2)$ the least squares estimate coincides with the maximum likelihood estimate.

An objective function with a simple sum of squares is often unsatisfactory. The size of the measurements may vary, here the tracee/tracer ratios are of order 10^{-3} and pool sizes are up to 10^2, or some measurements are less reliable than others. The solution to these two drawbacks to introduce weighted least squares. The weighted least squares is here defined as

$$\mathrm{O_{WLS}}(\mathbf{p}) = \sum_{i=1}^{m}\sum_{j=1}^{N_i} w_{i,j}(\phi_{i,j} - S_i(\mathbf{p}, t_{i,j}))^2, \tag{2.11}$$

for $w_{i,j} > 0$.

In every experiment there are errors $e_{i,j}$ in the measurements, so

$$\phi_{i,j} = S_i(\mathbf{p}, t_{i,j}) + e_{i,j}.$$

Assume that $E(e_{i,j}) = 0$ and that the variance of the error element $e_{i,j}$ is $\sigma_{i,j}$. There are several ways to deal with errors in the measurements. For instance one can give a weight to each term in the objective function according to the variance of the measurement. Let $w_{i,j} = 1/\sigma_{i,j}^2$ in 2.11.

$$\mathrm{O_{WLS}}(\mathbf{p}) = \sum_{i=1}^{m}\sum_{j=1}^{N_i}\left(\frac{\phi_{i,j} - S_i(\mathbf{p}, t_{i,j})}{\sigma_{i,j}}\right)^2.$$

If a point is measured with high accuracy, i.e. its variance is small, that data point will have a large weight in the objective function. An other common way of weight data is to weight each sample by $1/\phi_{i,j}^2$ (or $1/S_i(t_{i,j})^2$), which gives a penalty in terms of relative error rather than absolute error.
It can be assumed that the variance can written as

$$\mathrm{Var}(e_{i,j}) \quad = \quad \mathrm{V}_{i,j}(\phi_{i,j}, S_i(\mathbf{p}, t_{i,j}), v_j).$$

i.e. the variance depends on the sampled value $\phi_{i,j}$, the calculated value $S_{i,j}$ and a parameter v_j. v_j is a measure of how good the data set j are and may depend on the accuracy of the different methods used in the experiment. It is often assumed that the variance depends on $\phi_{i,j}$ or $S_{i,j}$, depending on weather it is believed that the model or data is more correct. v_j may depend on the method used for analysing the data.
As discussed in Section 2.8, in the software used to interpret the model the objective function also includes a logarithmic term of the weights. It is also possible to include a Baysian term in the objective function. There may exist some *a priori* information for some parameters. This may come from population average or from earlier experiment.

2.6.2 Search algorithms

After choosing a starting point $\mathbf{p}_0$ there are several approaches to find an optimal solution. In general, most search algorithms are based on the following; First a *search direction* is chosen, and then a *step length*. This is repeated until an optimum is reached. The most common are the *steepest descent* search direction; it finds the direction in which the greatest change of the objective function is achieved.

2.7 A four compartments example

Here is a simple example of a compartmental model. It is also the first attempt to model lipoprotein kinetics. The tracee in this model is the apoB, or even more specifically - the leucine amino acids in the apoB molecules. How the labelling is done and why leucine is chosen as the tracee is described in Section 3.1. The tracer is a stable isotope of leucine. Let Q_1 be the mass of free leucine in the blood and in the liver, let further Q_2, Q_3 and Q_4 be the mass of leucine in VLDL, IDL and LDL respectively. Denote the corresponding tracer masses by $q_i,\ i = 1, 2, 3, 4$. With external input of tracee from the environment and an instant injection of tracer into compartment 1. The compartmental system is shown in figure 2.5, and the equations describing the model are

$$\begin{aligned}
\mathbf{Q} &= \begin{pmatrix} Q_1 & Q_2 & Q_3 & Q_4 \end{pmatrix}^T, \\
\mathbf{q} &= \begin{pmatrix} q_1 & q_2 & q_3 & q_4 \end{pmatrix}^T, \\
\mathbf{U} &= \begin{pmatrix} U_0 & 0 & 0 & 0 \end{pmatrix}^T, \\
\dot{\mathbf{Q}}(t) &= \mathbf{K}\,\mathbf{Q}(t) + \mathbf{U}, \\
\dot{\mathbf{q}}(t) &= \mathbf{K}\,\mathbf{q}(t), \\
\mathbf{q}(0) &= \begin{pmatrix} q_0 & 0 & 0 & 0 \end{pmatrix}^T,
\end{aligned}$$

where q_0 is the injected mass. And

$$\mathbf{K} = \begin{pmatrix} -(k_{0,1}+k_{2,1}) & 0 & 00 & \\ k_{2,1} & -(k_{0,2}+k_{3,2}) & 0 & 0 \\ 0 & k_{3,2} & -(k_{0,3}+k_{4,3}) & 0 \\ 0 & 0 & k_{4,3} & -k_{0,4} \end{pmatrix}$$

Consider a steady state experiment with two measurements of total apoB in VLDL, IDL and LDL at 0 and 8 hours and 9 measurements of enrichment of free leucine, leucine in VLDL apoB and leucine in IDL and LDL apoB together (every hour). The outputs are defined as in figure 2.6 and 2.7, and the sampling matrices are

$$\mathbf{C} = \begin{pmatrix} 0 & 1 & 0 & 0 \\ 0 & 0 & 1 & 0 \\ 0 & 0 & 0 & 1 \end{pmatrix},$$

$$\mathbf{c} = \begin{pmatrix} 1 & 0 & 0 & 0 \\ 0 & 1 & 0 & 0 \\ 0 & 0 & 1 & 1 \end{pmatrix}.$$

For the tracee, the measurements s1, s2 and s3 (see figure 2.6) are denoted $\hat{\mathbf{S}}_j$, $j = 1, 2$ (0 and 8 hours) and corresponds to $\mathbf{CQ}(t)$. Similarly there are measurements s4, s5 and s6, for enrichment (see figure 2.7). The measurements are denoted $\hat{\mathbf{s}}_j$ where $j = 1, \ldots, 9$. For the tracer, $\hat{\mathbf{s}}$ corresponds to $\frac{\mathbf{cq}(t)}{\mathbf{cQ}(t)}$ (where the division is element by element). The least squares

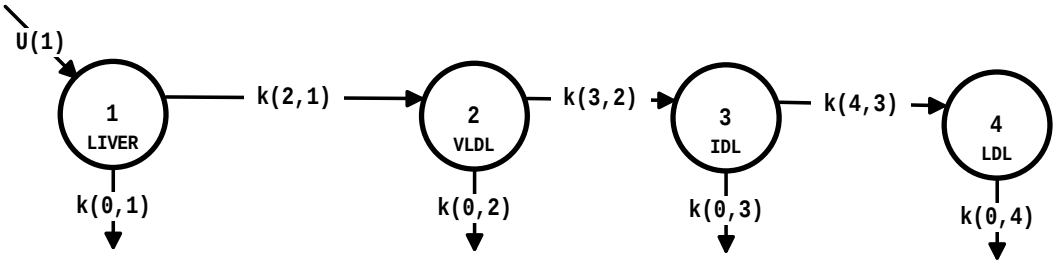

Figure 2.5: Compartmental model of the system.

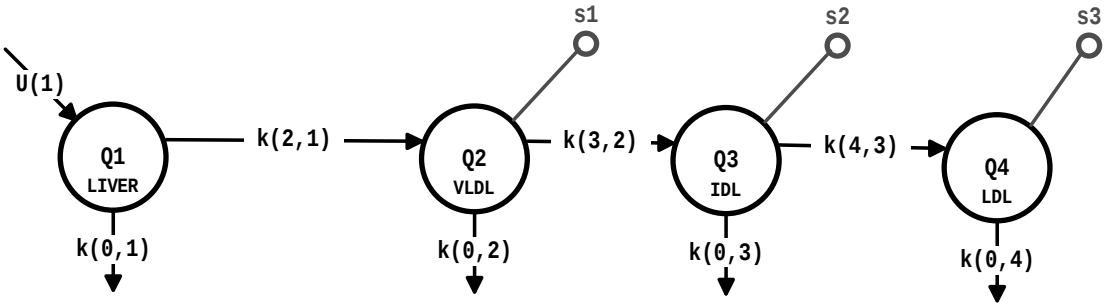

Figure 2.6: Tracee samples of VLDL, IDL and LDL at 0 and 8 hours.

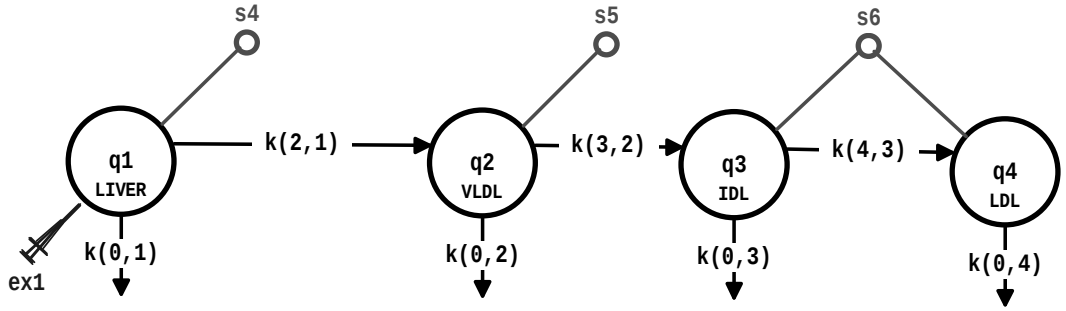

Figure 2.7: Enrichment of free tracer, tracer in VLDL and in IDL and LDL together.

objective function is

$$\mathrm{O_{LS}} \quad = \quad \sum_{j=1}^{2} \|\hat{\mathbf{S}}_j - \mathbf{CQ}(t_j^e)\|_2^2 + \sum_{j=1}^{9} \|\hat{\mathbf{s}}_j - \frac{\mathbf{cq}(t_j^r)}{\mathbf{cQ}(t_j^r)}\|_2^2.$$

In this case $t_1^e = 0,\ t_2^e = 8$ and $t_j^r = j - 1,\ j = 1, \ldots, 9$. A solution to this (minimising the errors as described in Section 2.6) may look as shown in figure 2.8.

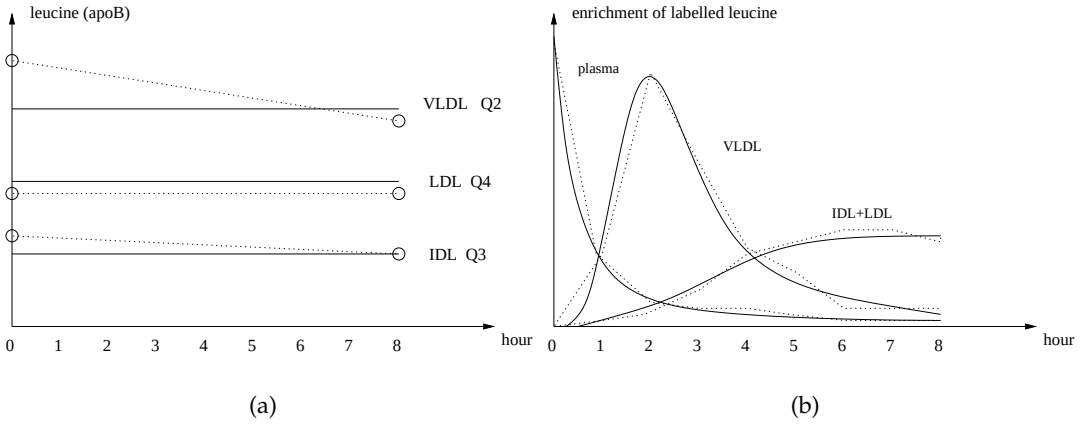

Figure 2.8: Possible solutions to the system, solid lines refer to calculated solutions and dashed lines to measured values. The error is the sum of squared differences between calculated and measured values.

2.8 Modelling software - The SAAMII program

In this thesis a commercially available program called **SAAMII** (*Simulation, Analysis And Modelling*) is used to create the model and perform the optimisation. SAAMII consist of a numerical and a compartmental module. The compartmental module has been used for the

modelling. A system is easily created by drawing compartments on the screen and transfer rates are assign by linking compartments together.
In SAAMII tracer/tracee experiment is then created by making a *system* (tracee) and a tracer experiment. The outputs are created as samples of the compartments and are associated with user data. Delays are modelled as a single component and implemented as described in Section 2.4.

2.8.1 Optimising in SAAMII

In SAAMII the objective function is a weighted least squares function with the variance as weights. The variance model is

$$\begin{aligned} Var(e_{i,j}) &= V_{i,j}(v_i, \phi_{i,j}, S_i(\mathbf{p}, t_{i,j})) \\ &= v_i\, \sigma_{i,j}. \end{aligned}$$

Where v_i is a measure of the set variance i.e how good the data set are. The objective function also includes a logarithmic term of the weights. Without such a term, the objective function could be arbitrary decreased by choosing parameters that increase the estimated variance.

$$\mathrm{O}_{\mathrm{SAAM}}(\mathbf{p}) = \frac{1}{M}\sum_{i=1}^{m}\sum_{j=1}^{N_i}\frac{(\phi_{i,j} - S_i(\mathbf{p}, t_{i,j}))^2}{V_{i,j}(v_i, \phi_{i,j}, S_i(\mathbf{p}, t_{i,j}))} + \log(V_{i,j}(v_i, \phi_{i,j}, S_i(\mathbf{p}, t_{i,j}))).$$

Where M is the total number of time points. There is also a possibility to use Baysian estimation of one or more parameters. If where are some parameters with a known mean and standard deviation (from earlier studies or population means) these parameters are being treated as an extra data set. The extra term in the objective function is

$$\sum_{k=1}^{N_b}(\frac{p_k - m_k}{\sigma_k})^2 + log(\sigma_k^2),$$

where p_k are the parameters, m_k their mean values and σ_k the standard deviation. N_b is the number of parameters being estimated with Baysian estimation.

2.8.2 Variance and weights

Variance model	based on data	based on model
Known standard deviation, d	$\sigma_{i,j} = d$	$\sigma_{i,j} = d$
Known fractional standard deviation, f	$\sigma_{i,j} = f\ \phi_{i,j}$	$\sigma_{i,j} = f\ S_i(\mathbf{p}, t_{i,j})$
Known poisson statics, r	$\sigma_{i,j} = \sqrt{r\ \phi_{i,j}}$	$\sigma_{i,j} = \sqrt{r\ S_i(\mathbf{p}, t_{i,j})}$
General formula, A, B, C	$\sigma_{i,j} = \sqrt{A + B\ \phi_{i,j}^C}$	$\sigma_{i,j} = \sqrt{A + B\ S_i(\mathbf{p}, t_{i,j})^C}$

Table 2.1: Variance models used by SAAMII, d, f, r, A, B, C are user supplied.

For the variance model, the eight combinations in table 2.1 are possible. The v_i component is estimated by

$$\hat{v}_i = \frac{1}{N_i}\sum_{j=1}^{N_i}\frac{(\phi_{i,j} - S_i(\mathbf{p}, t_{i,j}))^2}{V_{i,j}(1, \phi_{i,j}, S_i(\mathbf{p}, t_{i,j}))}.$$

For more information about SAAMII, visit *www.saam.com* or read [17].

Chapter 3

Lipoprotein experiment

This is a mathematical thesis, focusing on the mathematical model of lipoprotein metabolism. All clinical measurements and the analysis of blood samples are done by researchers and technichicans. The recruited subjects were all finish people. The samples were taken at the University Hospital in Helsinki, Finland, by Professor Marja-Riitta Taskinen and staff. All the analyses except for enrichments were done in Helsinki. The analysis for tracee/tracer ratios were carried out in The Royal Infirmary, Glasgow, UK, by Dr Muriel Caslake and staff. A short description of how the analyses were done is presented here.

3.1 Labelling of particles

In the studies, both the flow of particles and the flow of triglycerides were measured. Therefore the lipoproteins and the TG must be labelled individually. The particles were labelled by a bolus injection of labelled leucine (L-leucine-d_3, 7 mg/kg). The labelled leucine is, in the liver, used as material for apoB (the apoB molecule consists of 12.12% leucine, i.e. about 550 amino acids of leucine). The TG was labelled by a bolus injection of labelled glycerol (D-5-glycerol, 500 mg). In the liver, the labelled glycerol is inserted into the TG. Both L-leucine-d_3 and D-5-glycerol are stable isotopes.

3.2 Data

For each subject in the study the pool-sizes (total amount in plasma) of apoB and TG, were measured at 0, 4 and 8 hours in $VLDL_1$ and $VLDL_2$. From that the leucine in apoB and glycerol in TG were calculated. Moreover, the enrichments of labelled leucine and glycerol were measured at 0, 15, 30, 45, 60, 75, 90, 120, 150, 180, 240, 300, 360, 420 and 480 minutes in $VLDL_1$ and $VLDL_2$. Additionally measurements of enrichment of free leucine in plasma were done at 2, 6, 8, 10, 12, 15, 20, 30, 45, 60, 120, 180, 240 and 360 minutes. Let $t_{i,j},\ i = 1, 2, 6, 7$ be the time points for measurements of pool sizes in leucine $VLDL_1$, leucine $VLDL_2$, glycerol $VLDL_1$ and glycerol $VLDL_2$ ($N_i = 3,\ i = 1, 2, 6, 7$) and let $t_{i,j},\ i = 3, 4, 8, 9$ be the time points for measurement of enrichments of leucine $VLDL_1$, leucine $VLDL_2$, glycerol $VLDL_1$ and glycerol $VLDL_2$ ($N_i = 15,\ i = 3, 4, 8, 9$).
Finally let $t_{5,j}$ be the time points for enrichment of leucine in free plasma ($N_5 = 14$). This definition gives the possibility to exclude samples if some errors occurred during the analysis

of the plasma or in the experiment.

Name	time points		
$\phi_{1,j}$	$t_{1,j}$	$j = 1, \ldots, N_1$	total *leucine* in *apoB* VLDL_1 mass
$\phi_{2,j}$	$t_{2,j}$	$j = 1, \ldots, N_2$	total *leucine* in *apoB* VLDL_2 mass
$\phi_{3,j}$	$t_{3,j}$	$j = 1, \ldots, N_3$	enrichment of *labelled leucine* in *apoB* VLDL_1
$\phi_{4,j}$	$t_{4,j}$	$j = 1, \ldots, N_4$	enrichment of *labelled leucine* in *apoB* VLDL_2
$\phi_{5,j}$	$t_{5,j}$	$j = 1, \ldots, N_5$	enrichment of *labelled leucine* in *free leucine*
$\phi_{6,j}$	$t_{6,j}$	$j = 1, \ldots, N_6$	total *glycerol* in *TG* VLDL_1 mass
$\phi_{7,j}$	$t_{7,j}$	$j = 1, \ldots, N_7$	total *glycerol* in *TG* VLDL_2 mass
$\phi_{8,j}$	$t_{8,j}$	$j = 1, \ldots, N_8$	enrichment of *labelled glycerol* in *TG* VLDL_1
$\phi_{9,j}$	$t_{9,j}$	$j = 1, \ldots, N_9$	enrichment of *labelled glycerol* in *TG* VLDL_2

Table 3.1: Data sets.

3.3 Separation of densities and analysis of leucine and glycerol

The VLDL_1 and VLDL_2 were separated from plasma by cumulative flotation gradient ultra centrifugation. This method is described in [8], and only a brief description is given here. To the each sample (8.4 mL) 0.6 mL of NaCl (density $d = 1.019$ g/mL) was added and the samples were put in a centrifuge. Particles with density greater than $d = 1.019$ g/mL float up during the centrifugation and can then be separated from the plasma. A similar procedure was then applied to further separate the VLDL_1 and VLDL_2 particles.
To determine enrichment of labelled leucine, apoB molecules were separated (as described in [8]) and enrichment measured with gas chromatograph mass spectrometry. The method for measure enrichments of labelled leucine generally generates good data, whereas the method for labelled glycerol gives more noise and more spikes in the data.

3.4 Subjects

For the development of the model, 12 healthy subjects, nine normolipidemic and three with impaired glucose intolerance (IGT) was recruited. For the design of the model the nine normals was used. The subjects (the nine normolipidemic and one IGT, see Section 5) are further characterised in appendix A. The enrichments of apoB and TG are presented in figures A.1-A.10.

Chapter 4

Mathematical models

The apoB model was first developed, as it serves as a base for the glycerol model. As particles always are losing lipids their density is increasing monotonically. This gives a lower triangular system for the apoB and glycerol lipoprotein system. The model used for $VLDL_1$ and $VLDL_2$ apoB was first developed by C. J. Packard et al. [10]. The output compartments and corresponding functions are defined as in Section 2.3 and table 3.1.

4.1 apoB

A simple apoB model is described in Section 2.7. Now the model for the assembly of apoB molecules as well as the apoB $VLDL_1$ and $VLDL_2$ kinetics are described.

4.1.1 Liver-plasma leucine

The following model (figure 4.1) for liver-plasma apoB synthesis is described in [9]. The labelled leucine is injected into the plasma-leucine compartment (comp. 1), which is connected to a intracellular compartment (comp. 2). The fractional transfer coefficients between compartments 1 and 2 are equal, which gives an equilibrium between compartments 1 an 2. The intracellular compartment is the source for apoB synthesis. Compartments 3 and 4 are body protein pools accounting for uptake and slow release of leucine. Compartment 11 is the delay compartment (7 compartments for the delay is used, see Section 2.4). The sampled output is compartment 1, and $S_5(t)$ is defined as

$$S_5(t) = \frac{q_1(t)p_1}{Q_1(t)}.$$

The unknown proportion of plasma leucine that actually is in the plasma (not in liver etc) is denoted p_1.

4.1.2 $VLDL_1$

As described in Section 1.2, newly secreted particles in the $VLDL_1$ density are very TG-rich and undergo hydrolysis as the apoC activates the LPL. In the next step particles are either converted to $VLDL_2$ particles or removed by catabolism. In this model the particles enter the $VLDL_1$ fraction at one compartment. The model also allows for particles to be removed

from the hydrolysis-chain. Figure 4.2 shows the corresponding compartmental system. The VLDL_1 data described in Section 3.2 correspond to $Q_5 + Q_6 + Q_7$ (the tracee mass) and $\frac{q_5+q_6+q_7}{Q_5+Q_6+Q_7}$ (the tracer/tracee ratio) and

$$\begin{aligned} S_1(t) &= Q_5(t) + Q_6(t) + Q_7(t), \\ S_3(t) &= \frac{q_5(t) + q_6(t) + q_7(t)}{Q_5(t) + Q_6(t) + Q_7(t)}. \end{aligned}$$

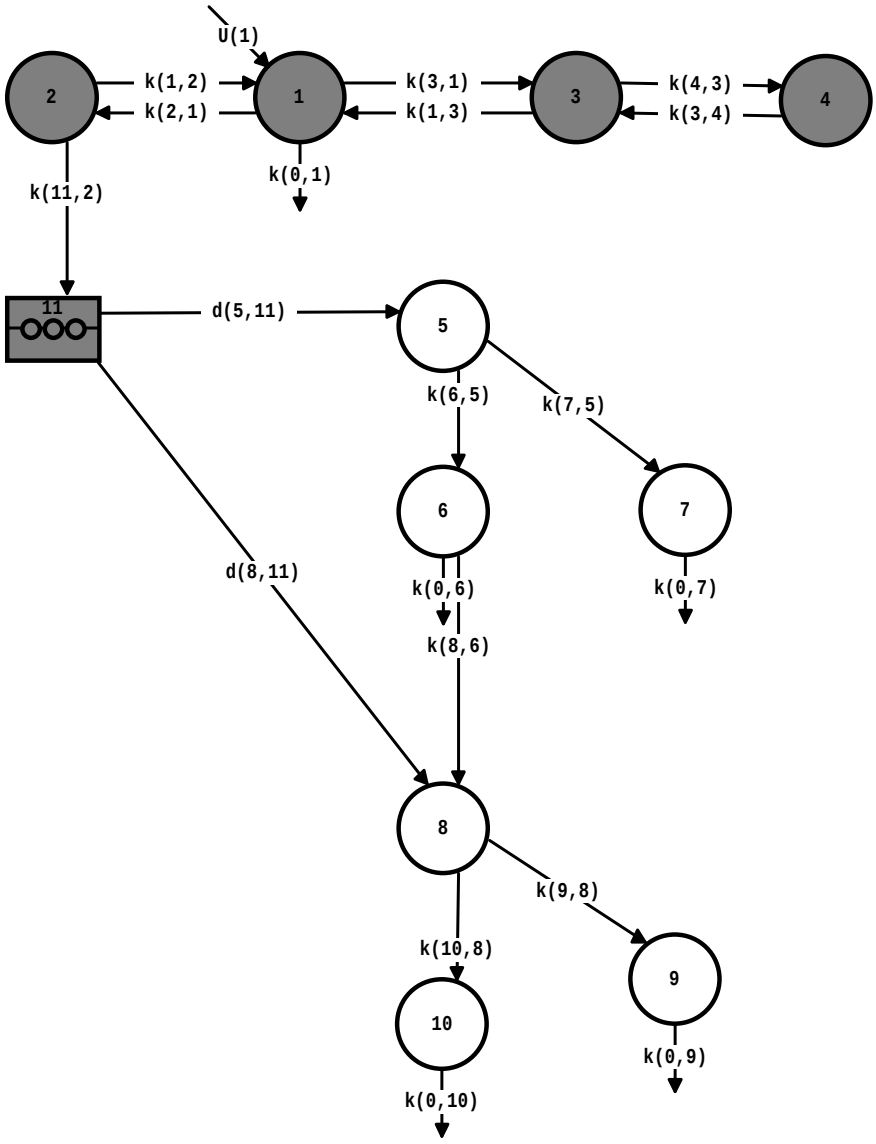

Figure 4.1: Liver-plasma. Compartment 1 is the plasma-leucine compartment where the leucine is injected. Compartment 2 is an intracellular compartment which is the source for apoB synthesis. Compartments 3 and 4 are body protein pools. The output is at compartment 1.

Compartments 5 and 6 are the delipidation chain and compartment 7 is the remnants compartment which allows for a slowly decaying component. There is a possibility for particles to be consumed by direct catabolism through compartment 6. The fractional transfer coefficient $k_{0,6}$ is initially set to 0. The fractional transfer coefficients in the delipidation chain are set to be equal, i.e. $k_{6,5} = k_{8,6}$.

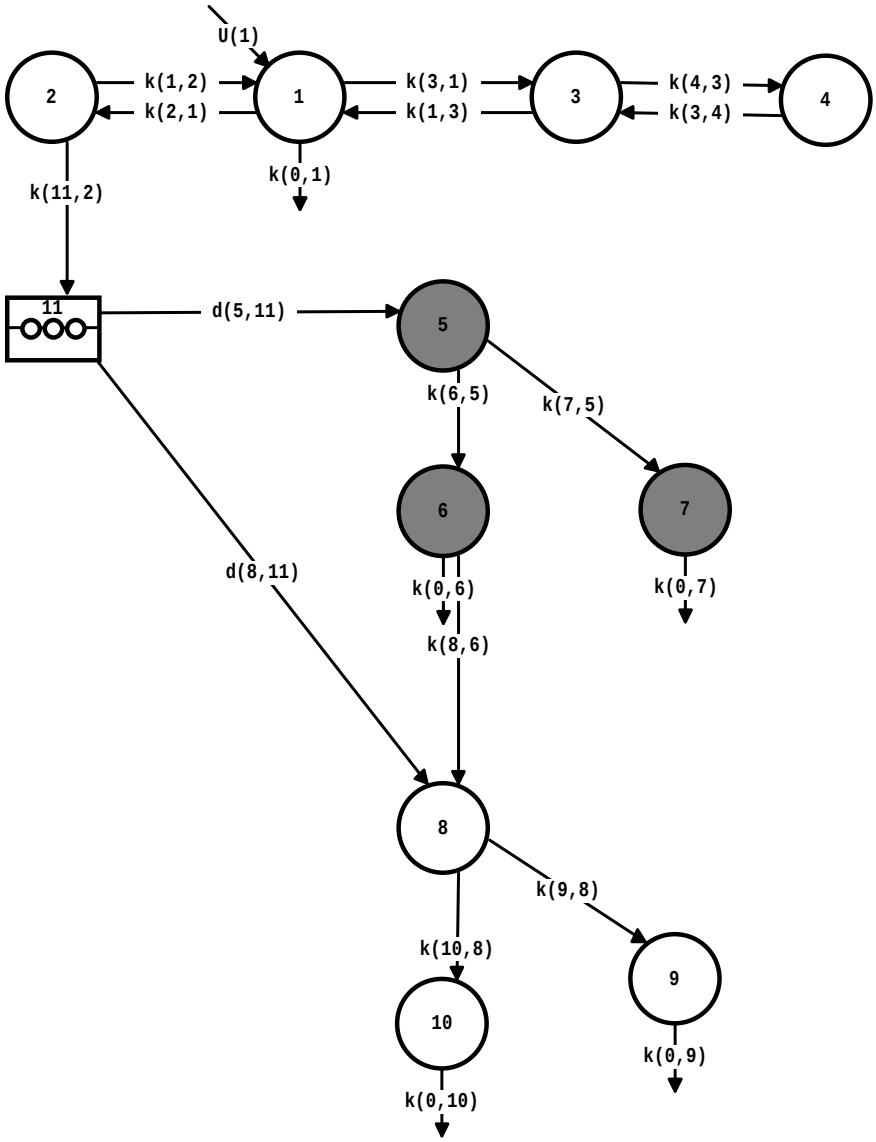

Figure 4.2: VLDL_1 . Compartments 5 and 6 are the delipidation chain and compartment 7 is the remnants compartment which allow for a slowly decaying component. The VLDL_1 output is the sum of compartments 5, 6 and 7.

4.1.3 VLDL$_2$

The VLDL$_2$ particles are described by a system similar to that of VLDL$_1$. For the normolipidemic subjects it was not necessary to use two distinct pathways. Particles coming from the liver can either be converted to IDL (through compartment 10) by further hydrolysis or they can be removed by catabolism (via the remnants compartment 9). In the model used here, particles coming from VLDL$_1$ can be removed by the same mechanism as newly secreted particles using compartment 9 in figure 4.3. Note that it is impossible to distinguish between catabolism and transfer to IDL from compartment 10, therefore $k_{0,10}$ is set to the sum of the transfer to IDL and the direct catabolism. Let $k_{0,10} = k_{10,8} + \mathrm{cat}_{10}$, where cat_{10}, the direct catabolism from compartment 10, is initially set to 0. Another possibility would be as in figure 4.4 where newly secreted particles are either cleared using compartment 13 or further hydrolysed with particles coming from VLDL$_1$. Using the model in figure 4.3 the VLDL$_2$ outputs are the sums of compartments 8, 9 and 10, giving the following functions

$$\begin{aligned} S_2(t) &= Q_8(t) + Q_9(t) + Q_{10}(t), \\ S_4(t) &= \frac{q_8(t) + q_9(t) + q_{10}(t)}{Q_8(t) + Q_9(t) + Q_{10}(t)}. \end{aligned}$$

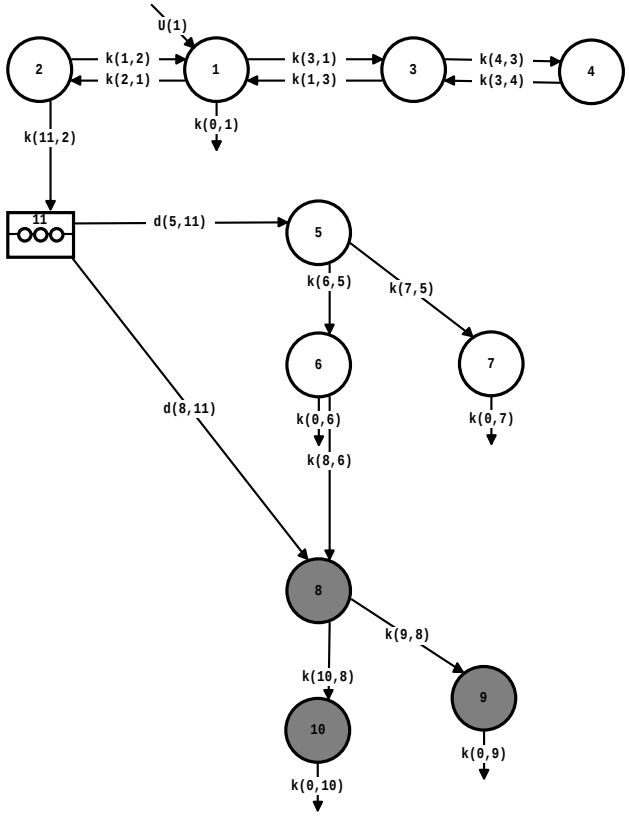

Figure 4.3: VLDL$_2$. The VLDL$_2$ system is similar to the VLDL$_1$ system. Compartments 8 and 10 are the delipidation chain and compartment 9 the remnants. The outputs of the VLDL$_2$ are the sums of compartments 8, 9 and 10.

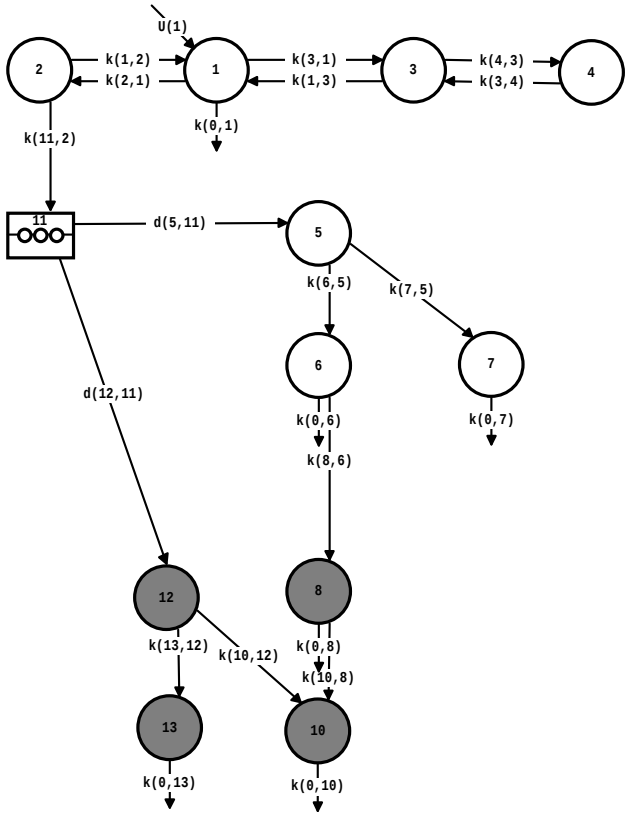

Figure 4.4: $VLDL_2$. An alternative, but not yet tested, system there compartments 8 and 10 are the delipidation chain. Particles coming direct from the liver (via comp. 12) may be transferred into the delipidation chain or become remnants (comp. 13). Here the $VLDL_2$ output would be the sum of compartments 8, 10, 12 and 13.

4.2 TG

The triglyceride model inherits most of the structure from the apoB model described above.

4.2.1 Liver-plasma

In the early paper by Loren A. Zech et al. [16] they presented a model for TG kinetic within the VLDL subclass. The model had a 5 compartment subsystem for the VLDL kinetics and 4+1 for the liver glycerol/TG conversion. Here a modified version of the liver model was used. Compartment 13 is the plasma-glycerol compartment where the glycerol is injected, and compartment 12 is a glycerol pool. Compartment 14 is the glycerol-TG conversion there compartment 21 is the slowly decaying compartment. The delay (comp. 22) is a 5 compartment delay initially set to 0.3 hours.
Other possible models could be to feed compartment 21 directly from compartment 12, and/or to feed compartment 21 into 22.

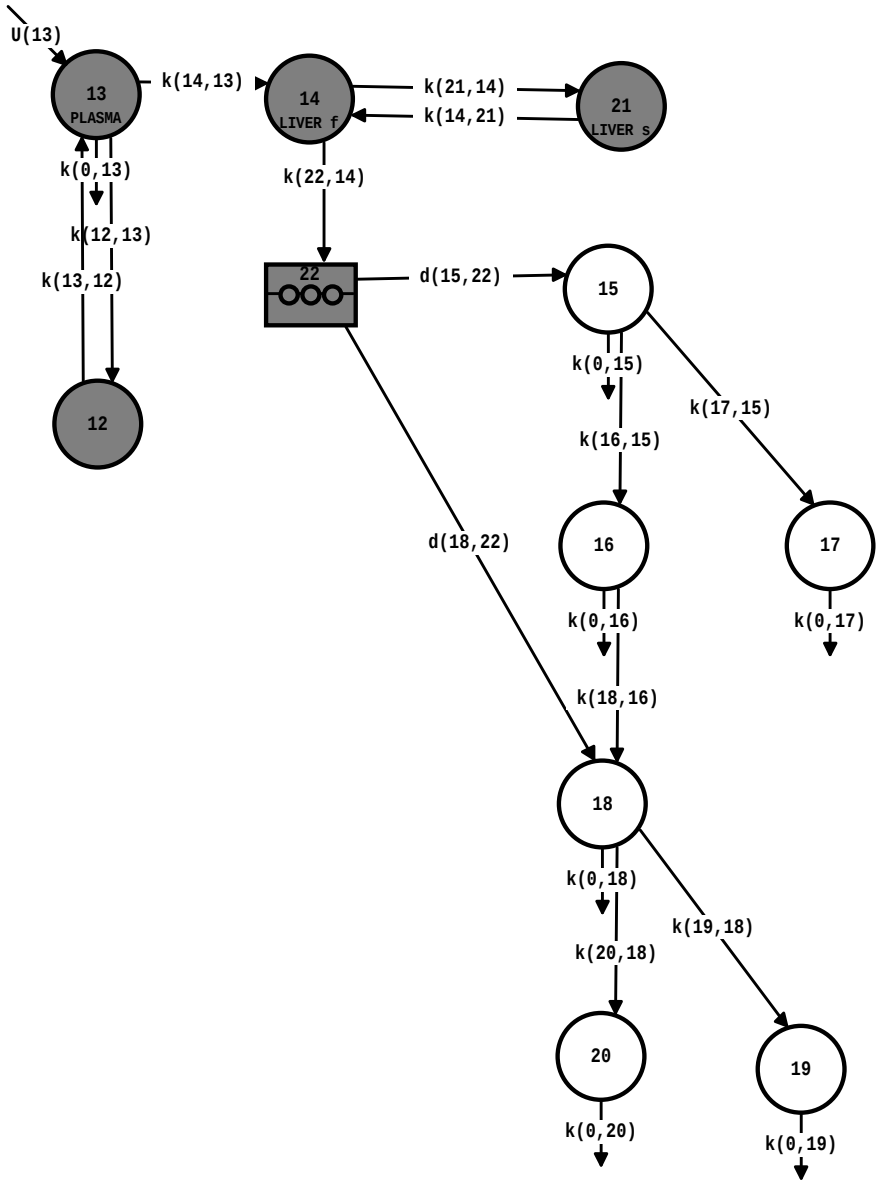

Figure 4.5: TG Liver system. Compartment 13 is the plasma-glycerol compartment and compartment 12 a glycerol pool. Compartments 14 and 21 are the fast and slow compartments respectively.

4.2.2 $VLDL_1$ and $VLDL_2$

The fractional transfer coefficients tells us the fraction of mass transferred per hour (or unit time). From the apoB model, the fraction of particles transferred is known, but if say 10% of the particles are transferred then 10% of the average TG mass is transferred as well. Therefore, for $VLDL_1$ and $VLDL_2$, the model for TG is almost the same as the model for apoB. The two models have the same structure with the same fractional transfer coefficients between compartments, but in each step lipids are lost so an additional loss term from each

compartment is added in the TG model. Compartments 16, 17, 18 and 20 have loss of TG both from catabolism of particles and hydrolysis. The outputs for $VLDL_1$ and $VLDL_2$ are the sums of compartments 15, 16 and 17 and 18, 19 and 20 respectively. The following functions

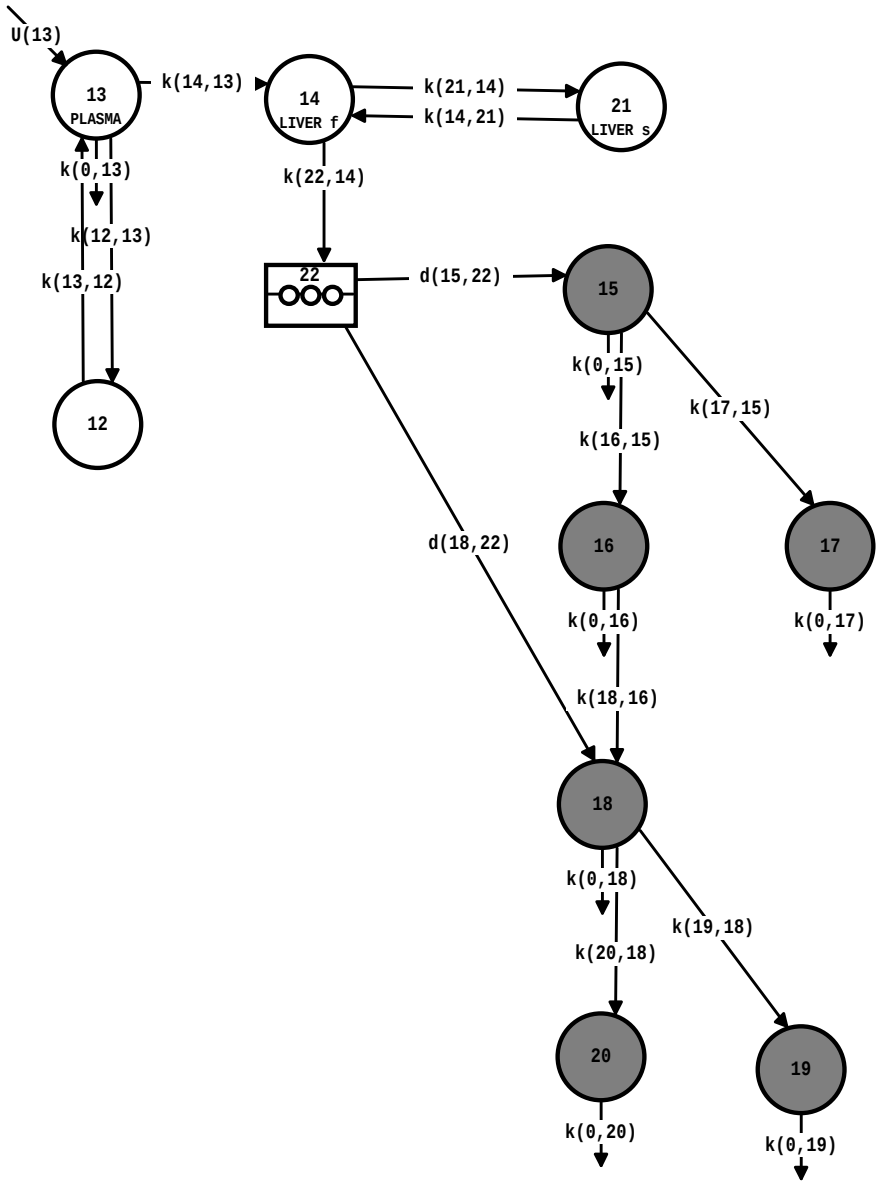

Figure 4.6: TG $VLDL_1$ and $VLDL_2$ system. The system is very similar to the apoB system. The outputs for $VLDL_1$ and $VLDL_2$ are the sums of compartments 15, 16 and 17 and 18, 19 and 20 respectively. Notice the loss $(k(0,i), i = 15, \ldots, 20)$ of TG from all VLDL compartments.

are therefore sampled

$$\begin{aligned} S_6(t) &= Q_{15}(t) + Q_{16}(t) + Q_{17}(t), \\ S_8(t) &= \frac{q_{15}(t) + q_{16}(t) + q_{17}(t)}{Q_{15}(t) + Q_{16}(t) + Q_{17}(t)}, \\ S_7(t) &= Q_{18}(t) + Q_{19}(t) + Q_{20}(t), \\ S_9(t) &= \frac{q_{18}(t) + q_{19}(t) + q_{20}(t)}{Q_{18}(t) + Q_{19}(t) + Q_{20}(t)}. \end{aligned}$$

4.3 Reduction of parameters - finding dependencies

In this chapter the number of unknowns is reduced to a minimum. When referring to a parameters such as $k_{2,3}$ the numbering of compartments as in figures 4.1 and 4.5 is used. From a computational point of view the number of unknown should be kept to a minimum in order to get faster and more efficient algorithms. In physiological terms reducing parameters is very critical, since by letting transfer-coefficients depend on each other the behavior of the model is partially determined. In the apoB liver model it is assumed that; $k_{1,2} = k_{2,1}$ and $k_{3,4} = k_{4,3}$ 0.1. For the TG liver model the parameter values as in [16] is used. As mentioned in Section 4.2.2 all fractional transfer coefficients between compartments are the same in the apoB and TG model i.e. $k_{j,i} = k_{j-10,i-10}$ for $(j,i) \in (16,15), (17,15), (18,16), (19,18), (20,18)$. There are also fractional losses of lipid $k_{0,i}$ for $i = 15, \ldots, 20$. These losses arise from direct catabolism of particles and hydrolysis. Therefore, for example, $k_{0,16} = k_{0,6} + L_6$ where L_6 is the loss from hydrolysis. The $k_{0,i}$ is bounded from below $k_{0,i} \geq k_{0,i-10}$ for $i = 15, \ldots, 20$ (if $k_{0,j}$ is not defined, $k_{0,j}$ is set to 0).

$$\begin{array}{rclrclrcl} k_{1,2} & = & k_{2,1} & k_{3,4} & = & k_{4,3}\ 0.1 & & & \\ k_{0,13} & = & 19 & k_{12,13} & = & 12 & k_{13,12} & = & 5 \\ & & & & & & & & \\ k_{8,6} & = & k_{6,5} & k_{0,10} & = & k_{10,8} + \mathrm{cat}_{10} & & & \\ & & & & & & & & \\ k_{16,15} & = & k_{6,5} & k_{17,15} & = & k_{7,5} & k_{18,16} & = & k_{8,6} \\ k_{20,18} & = & k_{10,8} & k_{19,18} & = & k_{9,8} & & & \\ & & & & & & & & \\ k_{0,15} & = & L_5 & k_{0,16} & = & k_{0,6} + L_6 & k_{0,17} & = & k_{0,7} + L_7 \\ k_{0,18} & = & L_8 & k_{0,19} & = & k_{0,9} + L_9 & k_{0,20} & = & k_{0,10} + L_{10} \end{array}$$

Table 4.1: Parameter dependencies and fixed parameters

4.4 Delays

When using the delay model described in Section 2.4, the resulting equation system is modified. Compartment 11 in figure 4.1 is an n_1 compartment delay, denote the compartments in the delay by $D_1^{\mathrm{apoB}}, \ldots, D_{n_1}^{\mathrm{apoB}}$ (and $d_1^{\mathrm{apoB}}, \ldots, d_{n_1}^{\mathrm{apoB}}$), and define the fractional transfer coefficient to be k_D^{apoB}. Further, define $F_{\mathrm{VLDL}_1}^{\mathrm{apoB}}$ to be the fraction of apoB mass that goes to the

VLDL_1 system, and $F^{\text{apoB}}_{\text{VLDL}_2} = 1 - F^{apoB}_{\text{VLDL}_1}$ the fraction that goes to the VLDL_2 system. Define

$$\mathbf{Q}^{\text{apoB}} = \begin{pmatrix} Q_1 & Q_2 & Q_3 & Q_4 & D_1^{\text{apoB}} & \cdots & D_{n_1}^{\text{apoB}} & Q_5 & \cdots & Q_{10} \end{pmatrix}^T,$$

and

$$\mathbf{q}^{\text{apoB}} = \begin{pmatrix} q_1 & q_2 & q_3 & q_4 & d_1^{\text{apoB}} & \cdots & d_{n_1}^{\text{apoB}} & q_5 & \cdots & q_{10} \end{pmatrix}^T.$$

This gives a system of the form

$$\begin{aligned} 0 &= \mathbf{K}^{\text{apoB}}\mathbf{Q}^{\text{apoB}} + \mathbf{U}^{\text{apoB}}, \\ \dot{\mathbf{q}}^{\text{apoB}} &= \mathbf{K}^{\text{apoB}}\mathbf{q}^{\text{apoB}}, \\ \mathbf{q}^{\text{apoB}}(0) &= \mathbf{q}_0^{\text{apoB}} = \begin{pmatrix} q_0^{\text{apoB}} & 0 & \cdots & 0 \end{pmatrix}^T, \end{aligned}$$

where $\mathbf{K}^{\text{apoB}}$ is defined as follows.

$$\mathbf{K}^{\text{apoB}} = \begin{pmatrix} \mathbf{K}^{\text{apoB}}_{\text{plasma}} & \mathbf{0} & \mathbf{0} \\ \mathbf{K}^{\text{apoB}}_{1} & \mathbf{K}^{\text{apoB}}_{\text{delay}} & \mathbf{0} \\ \mathbf{0} & \mathbf{K}^{\text{apoB}}_{2} & \mathbf{K}^{\text{apoB}}_{\text{VLDL}} \end{pmatrix},$$

where

$$\mathbf{K}^{\text{apoB}}_{\text{plasma}} = \begin{pmatrix} -k_{2,1} - k_{0,1} - k_{3,1} & k_{1,2} & k_{1,3} & 0 \\ k_{2,1} & -k^{\text{apoB}}_{delay} - k_{1,2} & 0 & 0 \\ k_{3,1} & 0 & -k_{1,3} - k_{4,3} & 0 \\ 0 & 0 & k_{4,3} & -k_{3,4} \end{pmatrix},$$

and

$$\mathbf{K}^{\text{apoB}}_{1} = \begin{pmatrix} 0 & k^{\text{apoB}}_{delay} & 0 & 0 \\ 0 & 0 & 0 & 0 \\ \vdots & \vdots & \vdots & \vdots \\ 0 & 0 & 0 & 0 \end{pmatrix},$$

which is an n_1 by 4 matrix.

$$\mathbf{K}^{\text{apoB}}_{\text{delay}} = \begin{pmatrix} -k_D^{\text{apoB}} & 0 & 0 & \cdots & 0 \\ k_D^{\text{apoB}} & -k_D^{\text{apoB}} & 0 & \cdots & 0 \\ 0 & \ddots & \ddots & \ddots & \vdots \\ \vdots & \ddots & k_D^{\text{apoB}} & -k_D^{\text{apoB}} & 0 \\ 0 & \cdots & 0 & k_D^{\text{apoB}} & -k_D^{\text{apoB}} \end{pmatrix},$$

is an n_1 by n_1 matrix. Moreover

$$\mathbf{K}^{\text{apoB}}_{2} = \begin{pmatrix} 0 & \cdots & 0 & F^{\text{apoB}}_{\text{VLDL}_1} k_D^{\text{apoB}} \\ 0 & \cdots & 0 & 0 \\ 0 & \cdots & 0 & 0 \\ 0 & \cdots & 0 & F^{\text{apoB}}_{\text{VLDL}_2} k_D^{\text{apoB}} \\ 0 & \cdots & 0 & 0 \\ 0 & \cdots & 0 & 0 \end{pmatrix},$$

is a 6 by n_1 matrix. Finally

$$\mathbf{K}^{\text{apoB}}_{\text{VLDL}} = \begin{pmatrix} -k_{6,5}-k_{7,5} & 0 & 0 & 0 & 0 & 0 \\ k_{6,5} & -k_{0,6}-k_{8,6} & 0 & 0 & 0 & 0 \\ k_{7,5} & 0 & -k_{0,7} & 0 & 0 & 0 \\ 0 & k_{8,6} & 0 & -k_{9,8}-k_{10,8} & 0 & 0 \\ 0 & 0 & 0 & k_{9,8} & -k_{0,9} & 0 \\ 0 & 0 & 0 & k_{10,8} & 0 & -k_{0,10} \end{pmatrix}.$$

Note that $\mathbf{K}^{\text{apoB}}$ plasma is the only matrix (on the diagonal of $\mathbf{K}$) that is not a lower triangular one. A model can be described with a lower triangular matrix if there is no feedback of material. In this model this means that particles are always moving downwards i.e. increasing their density.

4.5 The final model

The final apoB model is described in the Section above. The TG model is very similar. Compartment 22 in figure 4.5 is an n_2 compartment delay, denote the compartments in the delay by $D^{\text{TG}}_1, \ldots, D^{\text{TG}}_{n_2}$ (and $d^{\text{TG}}_1, \ldots, d^{\text{TG}}_{n_2}$), and define the fractional transfer coefficient to be k^{TG}_D. Define $F^{\text{TG}}_{\text{VLDL}_1}$ to be the fraction of TG mass that goes to the VLDL_1 system, and $F^{\text{TG}}_{\text{VLDL}_2} = 1 - F^{\text{TG}}_{\text{VLDL}_1}$ the fraction that goes to the VLDL_2 system. Define

$$\mathbf{Q}^{\text{TG}} = \begin{pmatrix} Q_{13} & Q_{12} & Q_{14} & Q_{21} & D^{\text{TG}}_1 & \cdots & D^{\text{TG}}_{n_2} & Q_{15} & \cdots & Q_{20} \end{pmatrix}^T,$$

and

$$\mathbf{q}^{\text{TG}} = \begin{pmatrix} q_{13} & q_{12} & q_{14} & q_{21} & d^{\text{TG}}_1 & \cdots & d^{\text{TG}}_{n_2} & q_{15} & \cdots & q_{20} \end{pmatrix}^T.$$

The system is of the form

$$\begin{aligned} 0 &= \mathbf{K}^{\text{TG}}\mathbf{Q}^{\text{TG}} + \mathbf{U}^{\text{TG}}, \\ \dot{\mathbf{q}}^{\text{TG}} &= \mathbf{K}^{\text{TG}}\mathbf{q}^{\text{TG}}, \\ \mathbf{q}^{\text{TG}}(0) &= \mathbf{q}^{\text{TG}}_0 = \begin{pmatrix} q^{\text{TG}}_0 & 0 & \cdots & 0 \end{pmatrix}^T. \end{aligned}$$

$\mathbf{K}^{\text{TG}}$ is defined as follows.

$$\mathbf{K}^{\text{TG}} = \begin{pmatrix} \mathbf{K}^{\text{TG}}_{\text{plasma}} & \mathbf{0} & \mathbf{0} \\ \mathbf{K}^{\text{TG}}_1 & \mathbf{K}^{\text{TG}}_{\text{delay}} & \mathbf{0} \\ \mathbf{0} & \mathbf{K}^{\text{TG}}_2 & \mathbf{K}^{\text{TG}}_{\text{VLDL}} \end{pmatrix},$$

where

$$\mathbf{K}^{\text{TG}}_{\text{plasma}} = \begin{pmatrix} -k_{12,13}-k_{14,13}-k_{0,13} & k_{13,12} & 0 & 0 \\ k_{12,13} & -k_{13,12} & 0 & 0 \\ k_{14,13} & 0 & -k_{21,14}-k^{\text{TG}}_{delay} & k_{14,21} \\ 0 & 0 & k_{21,14} & -k_{14,21} \end{pmatrix},$$

and

$$\mathbf{K}^{\text{TG}}_1 = \begin{pmatrix} 0 & 0 & k^{\text{TG}}_{delay} & 0 \\ 0 & 0 & 0 & 0 \\ \vdots & \vdots & \vdots & \vdots \\ 0 & 0 & 0 & 0 \end{pmatrix},$$

an n_2 by 4 matrix.

$$\mathbf{K}^{\mathrm{TG}}_{\mathrm{delay}} = \begin{pmatrix} -k_D^{\mathrm{TG}} & 0 & 0 & \cdots & 0 \\ k_D^{\mathrm{TG}} & -k_D^{\mathrm{TG}} & 0 & \cdots & 0 \\ 0 & \ddots & \ddots & \ddots & \vdots \\ \vdots & \ddots & k_D^{\mathrm{TG}} & -k_D^{\mathrm{TG}} & 0 \\ 0 & \cdots & 0 & k_D^{\mathrm{TG}} & -k_D^{\mathrm{TG}} \end{pmatrix},$$

is an n_2 by n_2 matrix, and

$$\mathbf{K}^{\mathrm{TG}}_{2} = \begin{pmatrix} 0 & \cdots & 0 & F^{\mathrm{TG}}_{\mathrm{VLDL}_1} k_D^{\mathrm{TG}} \\ 0 & \cdots & 0 & 0 \\ 0 & \cdots & 0 & 0 \\ 0 & \cdots & 0 & F^{\mathrm{TG}}_{\mathrm{VLDL}_2} k_D^{\mathrm{TG}} \\ 0 & \cdots & 0 & 0 \\ 0 & \cdots & 0 & 0 \end{pmatrix},$$

a 6 by n_2 matrix. Finally

$$\mathbf{K}^{\mathrm{TG}}_{\mathrm{VLDL}} = \begin{pmatrix} \begin{matrix} -k_{16,15}-k_{17,15} \\ -k_{0,15} \end{matrix} & 0 & 0 & 0 & 0 & 0 \\ k_{16,15} & -k_{0,16}-k_{18,16} & 0 & 0 & 0 & 0 \\ k_{17,15} & 0 & -k_{0,17} & 0 & 0 & 0 \\ 0 & k_{18,16} & 0 & \begin{matrix} -k_{19,18}-k_{20,18} \\ -k_{0,18} \end{matrix} & 0 & 0 \\ 0 & 0 & 0 & k_{19,18} & -k_{0,19} & 0 \\ 0 & 0 & 0 & k_{20,18} & 0 & -k_{0,20} \end{pmatrix}.$$

The relations between fractional transfer coefficients described in Section 3.2 imply that $\mathbf{K}^{\mathrm{TG}}_{\mathrm{VLDL}} = \mathbf{K}^{\mathrm{apoB}}_{\mathrm{VLDL}} + \mathbf{L}$, where

$$\mathbf{L} = \begin{pmatrix} -L_5 & 0 & 0 & 0 & 0 & 0 \\ 0 & -L_6 & 0 & 0 & 0 & 0 \\ 0 & 0 & -L_7 & 0 & 0 & 0 \\ 0 & 0 & 0 & -L_8 & 0 & 0 \\ 0 & 0 & 0 & 0 & -L_9 & 0 \\ 0 & 0 & 0 & 0 & 0 & -L_{10} \end{pmatrix}.$$

By the definition of the matrices $\mathbf{K}^{\mathrm{apoB}}$ and $\mathbf{K}^{\mathrm{TG}}$ they are irreducible and their longest circuits are of length 2, moreover they are open and hence all their eigenvalues are real and negative, according to Section 2.2. This means that there are no oscillations in solutions and the solutions are damped as time goes to infinity. There are no constant term in the solutions, and the tracer is completely washed out.

Chapter 5

Results

The subjects were chosen to have a wide spectrum of characteristics, in terms of bodyweight, TG-levels and age. The goal was to design a model that is applicable to as broad range of subject as possible. The nine normolipidemic and one of the IGT subjects were modelled. The other two IGT subjects were not possible to model with the developed model. Data for the ten subjects are presented in appendix A.

Each subject were modelled with the model described in Section 4 and the following quantities were calculated: the fractional catabolic rate **FCR**, the fractional direct catabolic rate **FDCR**, the direct production and the fractional transfer rate **FTR**. The formulas are presented in appendix B and calculated values in tables 5.2 and 5.3, the fractional transfer coefficients are presented in tables A.3 - A.6.

5.1 Optimisation

Due to the structure of the model the optimisation can be performed in a stepwise way. The model as in Section 4 was implemented in SAAMII with the parameters dependencies as in table 4.1 and 5.1. The data was weighted with relative weights, and was set to be 1% of the data point for the enrichments, and 10% for the pools.

5.1.1 Plasma apoB

First the optimisation was performed over the parameters associated with the plasma, namely p_1, plasmaLeucine, $k(0,1),\ k(1,2),\ k(1,3)$ and $k(4,3)$. The outflow of particles, $k(11,2)$, was kept constant. The objective is only to fit $S_5(t)$ to the points in $\phi_{5,j}$ at $t_{5,j},\ j = 1,\ldots,N_5$.

5.1.2 VLDL_1 and VLDL_2 apoB

Now the $k(1,2),\ k(2,1)$ and $k(4,3)$, and parameters dependent on these as in table 4.1, are fixed. The adjustable parameters are p_1, plasmaLeucine, $k(0,1)$, $k(0,6)$, $k(0,7)$, $k(0,9)$, $k(6,5)$, $k(7,5)$, $k(9,8)$, $k(10,8)$, $k(11,2)$, delayTime, $F^{\mathrm{apoB}}_{\mathrm{VLDL}_2}$ and cat_{10}. The objective is to fit $S_i(t)$ to $\phi_{i,j}$ at $t_{i,j},\ i = 1,\ldots,5,\ j = 1,\ldots,N_i$. For most of the subjects $k(0,6)$ and cat_{10} were zero. Therefore $k(0,6)$ and cat_{10} were initially set to 0. If necessary they were increased until a fit was achieved. Once a fit was found, the plasma parameters mentioned in Section 5.1.1 were

name	interval	description
p_1	$[0, 1]$	Unknown proportion of Q_1 measured
L_i	$[0, 6]$	Loss due to hydrolysis from $Q_i,\ i = 5, \ldots, 10$
$F^{\text{apoB}}_{\text{VLDL}_2}$	$[0, 1]$	Fraction of particles secreted as VLDL_2 particles
$F^{\text{TG}}_{\text{VLDL}_2}$	$[0, 1]$	Fraction of TG secreted in the VLDL_2 subfraction
delayTime	$[0.3, 0.8]$	Delay time for the apoB
delayTimeTG	$[0.1, 0.4]$	Delay time for the TG
$k(0, 1)$	$[0, 7]$	Fraction catabolised from 1
$k(0, 6)$	$[0, 3]$	Fraction catabolised from 6
$k(0, 7)$	$[0, 3]$	Fraction catabolised from 7
$k(0, 9)$	$[0, 3]$	Fraction catabolised from 9
cat_{10}	$[0, 3]$	Fraction catabolised from 10
$k(1, 2)$	$[0, 10]$	Fraction transferred from 2 to 1
$k(1, 3)$	$[0, 10]$	Fraction transferred from 3 to 1
$k(3, 1)$	$[0, 10]$	Fraction transferred from 1 to 3
$k(4, 3)$	$[0, 10]$	Fraction transferred from 3 to 4
$k(6, 5)$	$[0, 3]$	Fraction transferred from 5 to 6
$k(7, 5)$	$[0, 3]$	Fraction transferred from 5 to 7
$k(9, 8)$	$[0, 3]$	Fraction transferred from 8 to 9
$k(10, 8)$	$[0, 3]$	Fraction transferred from 8 to 10
$k(11, 2)$	$[0, 0.1]$	Fraction transferred from 2 to 11
$k(14, 13)$	$[0, 0.5]$	Fraction transferred from 13 to 14
$k(14, 21)$	$[0, 10]$	Fraction transferred from 21 to 14
$k(21, 14)$	$[0, 10]$	Fraction transferred from 14 to 21
$k(22, 14)$	$[0, 5]$	Fraction transferred from 14 to 22
plasmaGlycerol	$[50, 5000]$	Amount of free glycerol in plasma
plasmaLeucine	$[50, 5000]$	Amount of free leucine in plasma

Table 5.1: Adjustable parameters. plasmaLeucine will be the mass in compartment 1, and plasmaGlycerol the mass in compartment 13. Other parameters are as in table 4.1.

made adjustable and the optimisation was repeated - but little or no improvement of the fit was achieved.

5.1.3 TG

After achieving an optimum for the apoB model, the next step is to optimise over the TG model. All apoB parameters are fixed and the adjustable parameters are $L_i,\ i = 5, \ldots, 10$, $k(14, 13)$, $k(14, 21)$, $k(21, 14)$, $k(22, 14)$, $F^{\text{TG}}_{\text{VLDL}_2}$ and delayTimeTG. The objective is to fit $S_i(t)$ to $\phi_{i,j}$ at $t_{i,j},\ i = 6, \ldots, 9,\ j = 1, \ldots, N_i$. In general the data for enrichment of labelled glycerol were not as good as the data for labelled leucine.

5.1.4 Iterating

The TG model is based on the apoB model, which indicates that the apoB model should be optimised first and then the TG model. The two reasons for this are;

The apoB model has been tested in several studies, for instance [8], [10] and [9].
The techniques for the measurements of apoB are more accurate than those of TG, therefore a better fit for the apoB model than for the TG model can be predicted.
Some difficulties occurred during the optimisation. The problem occurred when modelling the TG, but the problem originated from the apoB solution. The two most common problems were

1. Delay time. The delay time for the apoB was in some subjects slightly large, due to a large weight of the first measurements of the enrichment. In the model this results in a high production rate, and therefore a large **FCR**. A lower weight for the first measurement gave a shorter delay time and produced a better fit.

2. $k(0,6)$. As mentioned earlier, the direct catabolism from compartment 6 was initially set to 0. If no feasible fit was achieved it was allowed to vary. This often resulted in a very large $k(0,6)$. Therefore $k(0,6)$ was defined to be the least $k(0,6)$ to produce a feasible fit.

	$VLDL_1$				$VLDL_2$					
subject	FCR	FDCR	FTR	Prod	FCR	Prod	Dprod	Tprod	$F^{\mathrm{TG}}_{\mathrm{VLDL}_1}$	dT
1	26,69	22,21	4,48	39452	17,12	9256	2631	42084	0,94	0,32
2	24,15	22,45	1,70	29620	13,51	5338	3251	32872	0,90	0,40
3	17,09	13,73	3,36	12108	8,98	3292	913	13021	0,93	0,32
4	8,04	6,39	1,65	11668	5,00	4119	1721	13389	0,87	0,29
5	16,85	16,20	0,66	55763	9,62	10074	7899	63662	0,88	0,21
6	37,56	30,78	6,78	19486	13,69	5283	1764	21250	0,92	0,33
7	32,84	22,69	10,15	31969	32,21	14077	4192	36162	0,88	0,28
8	54,24	45,97	8,27	40156	35,50	7685	1563	41719	0,96	0,20
9	13,12	11,06	2,06	29956	9,07	6585	1879	31835	0,94	0,40
10	15,20	11,57	3,63	22461	10,58	6962	1596	24056	0,93	0,23
mean	24,58	20,30	4,27	29264	15,53	7267	2741	32005	0,92	0,30
stderr	13,15	10,94	2,99	12955	9,70	3038	1943	14498	0,03	0,07

Table 5.2: Calculated TG values for subjects. Prod, production; Dprod, direct production; Tprod, total production; dT, delayTimeTG. FCR, FDCR and FTR [pools/day]; Prod, Dprod, Tprod [mg].

	$VLDL_1$				$VLDL_2$					
subject	FCR	FDCR	FTR	Prod	FCR	Prod	Dprod	Tprod	$F^{\mathrm{apoB}}_{\mathrm{VLDL}_1}$	dT
1	15,15	6,72	8,43	889	6,71	619	124	1013	0,88	0,46
2	16,53	11,75	4,78	799	5,98	409	178	977	0,82	0,48
3	12,74	8,22	4,53	383	3,53	231	95	478	0,80	0,73
4	6,22	3,23	2,98	275	2,13	219	87	363	0,76	0,45
5	5,93	3,29	2,64	840	4,19	655	281	1121	0,75	0,47
6	31,50	23,82	7,68	1078	6,29	523	260	1338	0,81	0,51
7	14,53	5,97	8,56	580	6,68	494	152	733	0,79	0,48
8	28,33	7,17	21,16	683	10,42	762	252	934	0,73	0,54
9	8,10	1,76	6,34	628	6,28	631	139	767	0,82	0,48
10	9,42	0,00	9,42	695	5,43	855	160	855	0,81	0,58
mean	14,85	7,19	7,65	685	5,76	540	173	858	0,80	0,52
stderr	8,79	6,77	5,31	237	2,23	209	69	290	0,04	0,08

Table 5.3: Calculated apoB values for subjects. Prod, production; Dprod, direct production; Tprod, total production; dT, delayTime. FCR, FDCR and FTR [pools/day]; Prod, Dprod, Tprod [mg].

Chapter 6

Discussion

6.1 Expected Values

There are many biological as well as mathematical considerations to be made when proposing a model. Though it is not a guarantee for the model to be correct, it is advisable to start by considering whether the results are physiologically possible.
Rough bounds for some quantities can be calculated and be compared to other studies.
$VLDL_1$ are richer in TG than $VLDL_2$ so clearly the fraction of TG going to $VLDL_1$ ($F^{\mathrm{TG}}_{\mathrm{VLDL}_1}$) should be greater than the fraction of apoB ($F^{\mathrm{apoB}}_{\mathrm{VLDL}_1}$), equality should hold if and only if both are 1 or 0.
There are many studies on apoB metabolism. In for instance [8], [9] and [13] values of $50 - 80\%$ of apoB to $VLDL_1$ are normal, and $70 - 80\%$ are most common. There are not many studies done on $VLDL_1$ and $VLDL_2$ TG metabolism, but some rough calculations can be made. Since the model only includes apoB and TG, only the ratio TG:apoB (see subject data in appendix A) can be considered. Newly produced particles are rich in TG and hence their TG:apoB ratio should be greater then the average ratio of the pools. Now apparently in table A.7 the TG:apoB ratio for newly secreted $VLDL_2$ particles are greater than the average $VLDL_1$ ratio for some subjects. This is probably because new $VLDL_2$ particles has low apoE and apoC as well as cholesterol content and their TG content may therefore vary within a certain density interval. The cholesterol is transferred from HDL to apoB-containing lipoproteins by cholesterol ester transfer protein, CETP, [15].

6.2 Delay times

There is a big difference in delay times between apoB and TG. For apoB the delay time is 0.52 ± 0.07 hours (31 minutes), whereas for TG it is 0.30 ± 0.08 hours (18 minutes). This indicates that the TG is added late in the synthesis of the lipoprotein.

6.3 $VLDL_1$ and $VLDL_2$ sizes

The newly secreted $VLDL_1$ particles are 2 times as rich in TG as the average $VLDL_1$ particle (43 to 25), but the newly secreted $VLDL_2$ particles have 3 times as much TG then the average $VLDL_2$ particle (16 to $5,7$). 92% of the TG is secreted into the $VLDL_1$ subfraction. These

facts indicates that most of the VLDL particles secreted from the liver have high TG to apoB content - $VLDL_2$ particles are secreted in the lower density region of the $VLDL_2$ subfraction.

6.4 Numerical results

The plasma was successfully fitted in all subjects except for subject 8. Subject 8 had a hump in the data between 1 and 3 hours, these points were excluded during the optimisation. The results for subject 8 might not be relevant, in table A.2 the TG to apoB ratio in $VLDL_1$ is above 40 at 0 hours, and is very high at 4 and 8 as well. The TG to apoB ratio in $VLDL_2$ is very low. This indicates that subject 8 might not by a normolipidemic.
Good fits for the apoB model were achieved for all the subjects. The apoB model was also successfully applied to a total of 21 subjects (not presented here). The solutions are presented as solid lines in figures A.1-A.10, in appendix A.
In subjects 2, 5 and 9 there is a 'hump' in the apoB, $VLDL_2$ data at approximately 1 hour. Since the solutions are sums of exponentials it is impossible to achieve such a hump in the solution. For subject 6 the data point at 6 hours for $VLDL_2$ is almost 0, and was left out during the optimisation. In some subjects, at some time points, the $VLDL_1$ and $VLDL_2$ were either slightly to close (as in subject 2 at 5 hours) or to much apart. This may indicate that there has been a problem with the separation of $VLDL_1$ and $VLDL_2$. Such time points have been left out during the optimisation. Another possibility would be to fit the total enrichment of $VLDL_1$ and $VLDL_2$ to the weighted sum of the data points, where the weights are the average pool sizes.
For the TG the data is not as good as for the apoB. For $VLDL_1$ the data are fairly good, but for $VLDL_2$ there is some noise. In for instance the subject 4 and 5 the $VLDL_2$ data are very noisy.

Chapter 7

Further development

7.1 The present model

There are two main improvements to be made to the present model. First, the time independent model will be further developed to be applicable to subjects with IGT and type-2 diabetes as well. When the current model was applied to IGT subjects it turned out that the enrichment of TG in $VLDL_2$ was not always possible to model. The enrichment for $VLDL_2$ grows for a longer period of time - and hence the peak for $VLDL_2$ comes later than for the normolipidemic subjects. This phenomenon is probably more noticeable in the type-2 diabetes subjects. The inflow of particles to $VLDL_2$ comes both from $VLDL_1$ and from the liver. In the current model $VLDL_2$ particles are supposed to have the same kinetics, independent of their origin. If the pathways for these particles were separated, the liver would produce a fast growing and decaying curve for $VLDL_2$. $VLDL_2$ from $VLDL_1$ would be a more slowly growing curve, since it is fed from $VLDL_1$.
The next step will be to make a time dependent model, to study the effect of insulin on apoB and TG secretion. Insulin is known to lower TG levels. Insulin regulates the availability of free fatty acids (FFA) in the liver. In [8], a constant insulin injection was shown to lower the apoB $VLDL_1$ production by 48%. Hence, $VLDL_1$ and $VLDL_2$ production can be regulated independently. Insulin also alter the removal of lipoproteins by its effect on the LPL.
In the new model it will be possible to study not only how the secretion of particles are affected by insulin but also how the composition is altered.

7.2 Other models

Apart from the improvements and modifications possible in the current model, e.g. the time dependence in the insulin model, and the IGT/diabetes modifications, other mathematical approaches to model are also possible.
In reality, there is a continuous distribution of particles with different densities, and the natural continuation of the project is to build a continuous simulation model. Such a model could be done in a stochastic way, where each particle is modelled individually.
A continuous model will be more flexible and more easily allow to include new information about the different metabolism at different densities. Apart from being useful in its own right, such a model will make it possible to evaluate compartmental models under fully controlled situations.

The synthesis in the liver could also be modelled with this probabilistic approach. For instance, the addition of triglycerides to the lipoprotein could be modelled in this way. A model like this could give information about the density spectrum of particles secreted from the liver. A question to adress is whether there are two distinct peaks for $VLDL_1$ and $VLDL_2$ or is the spectrum smooth? With a statistical model, or any continuous model, it would be possible to test the subdivision of VLDL to $VLDL_1$ and $VLDL_2$. Is the metabolic heterogeneity of particles in VLDL fixed or can it vary within the population or between normolipidemic and IGT/type-2 diabetes subjects? The idea is to fit the model to the measurements available but let the metabolic difference in VLDL be more or less independent of the subdivision into $VLDL_1$ and $VLDL_2$.
If the difference of the real subdivision of VLDL and the subdivision $VLDL_1$ and $VLDL_2$ is small, this could be tested in the compartmental model. For instance, the $VLDL_1$ data could be fitted to $Q_5+Q_7+(1-\alpha)\ Q_6+\beta\ Q_8$ and the $VLDL_2$ data fitted to $\alpha Q_6+(1-\beta)\ Q_8+Q_9+Q_{10}$ (the tracer/tracee ratios are defined in a similar way), where $\alpha\beta = 0,\ \alpha \geq 0$ and $\beta \geq 0$.

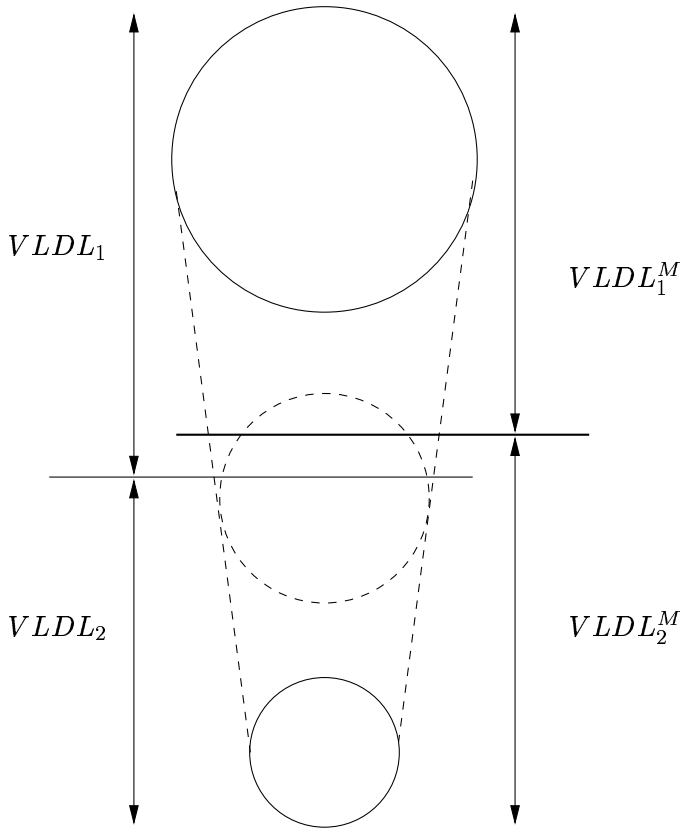

Figure 7.1: In a continuous model, the subdivision of VLDL into $VLDL_1$ and $VLDL_2$ could be tested by fitting the model to the data available ($VLDL_1$ and $VLDL_2$), but the metabolic difference is in the $VLDL_1^M$ and $VLDL_2^M$.

7.3 Statistical problems related to compartmental modelling

There are several statistical problems related to tracer experiments and compartmental models.
In the model it is assumed that the labelled particles are uniformly distributed among all the particles. Depending on how large proportion of particles that actually are labelled, the distribution might not be uniform.
When normal, IGT and type-2 diabetes subjects are modelled it is possible to investigate what differences and what similarities there are between these groups. For the insulin study the same subjects are recruited, so there is a good statistical material to study the effect of insulin.
The errors of the data has not been fully investigated. There are two ways of measuring apoB mass, direct measurement or by measuring the total protein content and the mass of non-apoB protein. Here the direct measurements of apoB has been used. Other possible approaches are to weight the apoB mass by the total protein mass divided by the sum of apoB and non apoB proteins. This gives a "recovery corrected" apoB mass.
The experiments are far from easy to carry out, and are affected by rather large errors. Many enrichments are measured from the same blood sample, and therefore the errors cannot be considered to be independent.
It might also be the case that is it possible to make assumptions on the errors and the variance of the data, depending on the different method used. But this is beyond the scope of this thesis.
The stability of the model has not been investigated. The model should be tested for changes in the data. The variance of both the output of the model, such as the FCR and production, and estimated parameters should be investigated, also how sensitive the output is to changes in the parameters.

Appendix A

Subject data

Subject	age	weight	BMI	BF	Insulin	TG	chol	HDL	FFA-0	LF
1	64	90,0	27,2	29,5	7,79	1,57	4,49	0	714	0
2	53	90,5	27,9	26,8	7,00	1,02	4,40	1,25	413	0
3	56	80,3	27,8	24,2	2,80	1,22	4,68	1,51	530	5
4	47	75,2	26,3	24,2	4,79	2,23	7,51	1,54	588	1
5	55	84,0	16,5	24,3	6,00	1,98	4,60	0	357	0
6	59	92,3	30,1	27,5	7,00	1,19	5,32	1,56	549	3
7	45	69,8	24,1	17,2	3,25	1,86	6,36	1,19	598	2
8	49	71,5	24,0	20,3	6,41	1,44	5,66	0	606	0
9	57	95,9	25,9	28,1	9,00	1,24	4,01	0	461	0
10	52	71,9	24,0	19,5	8,00	2,00	5,30	0	542	2
mean	54	82,1	25,4	24,1	6,20	1,57	5,23	0,71	536	1,3
stderr	6	9,7	3,7	4,0	2,03	0,42	1,06	0,75	103	1,7

Table A.1: Subject characteristics, total number of subjects = 10. BMI, Body Mass Index $(\mathrm{weight}/\mathrm{lenght}^2)$ [kg/m^2]; BF, Body Fat [%]; LF, Liver Fat [%].

The enrichment of apoB and TG is presented as '$\bullet$' and '$\circ$' respectively. The TG data are scaled so that the maximum of apoB and TG VLDL_1 are the same. The solid lines are the calculated enrichments.

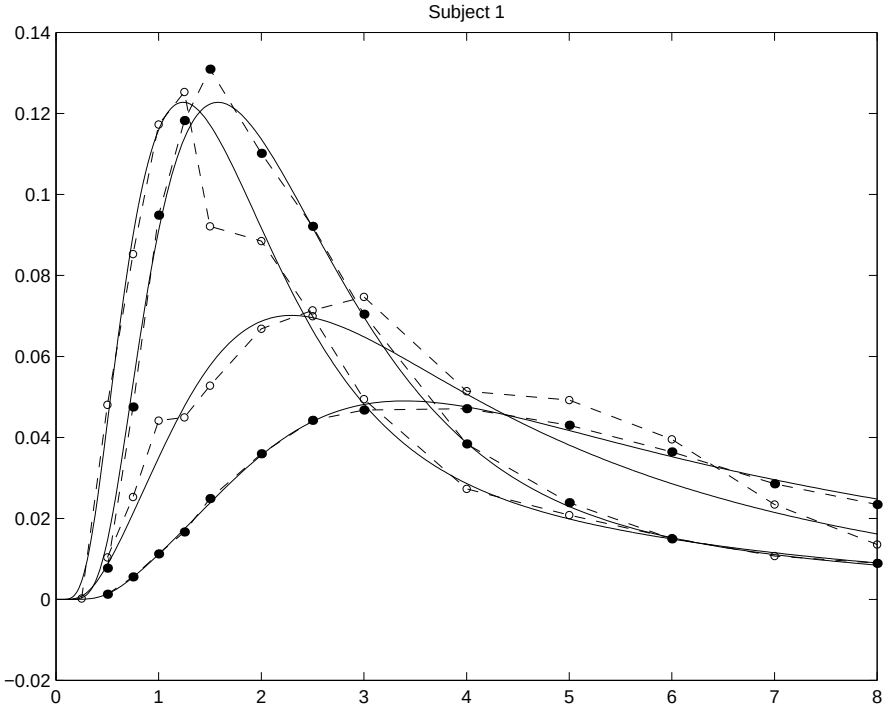

Figure A.1: Subject 1

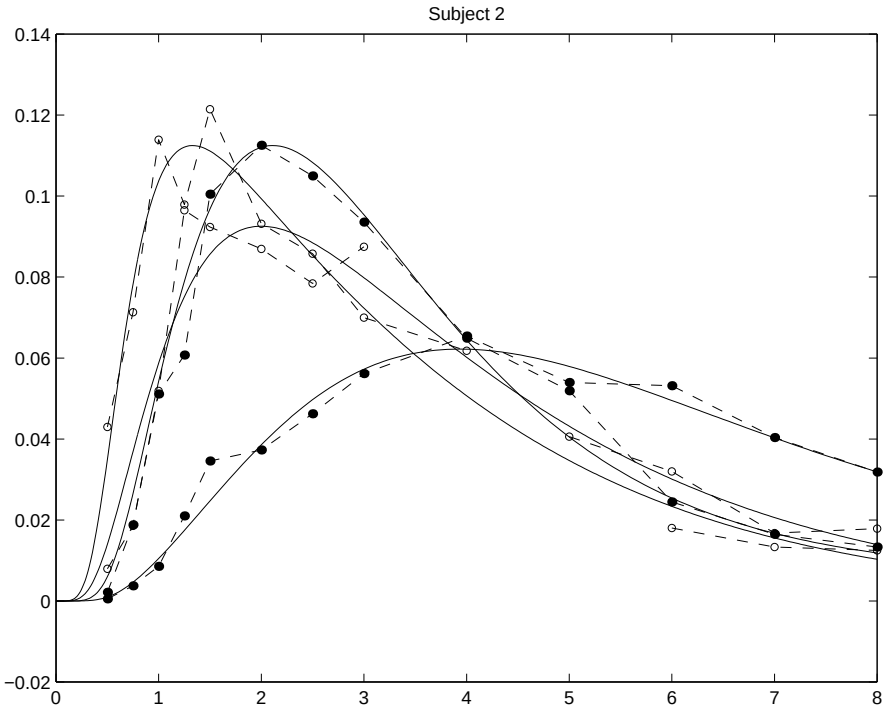

Figure A.2: Subject 2

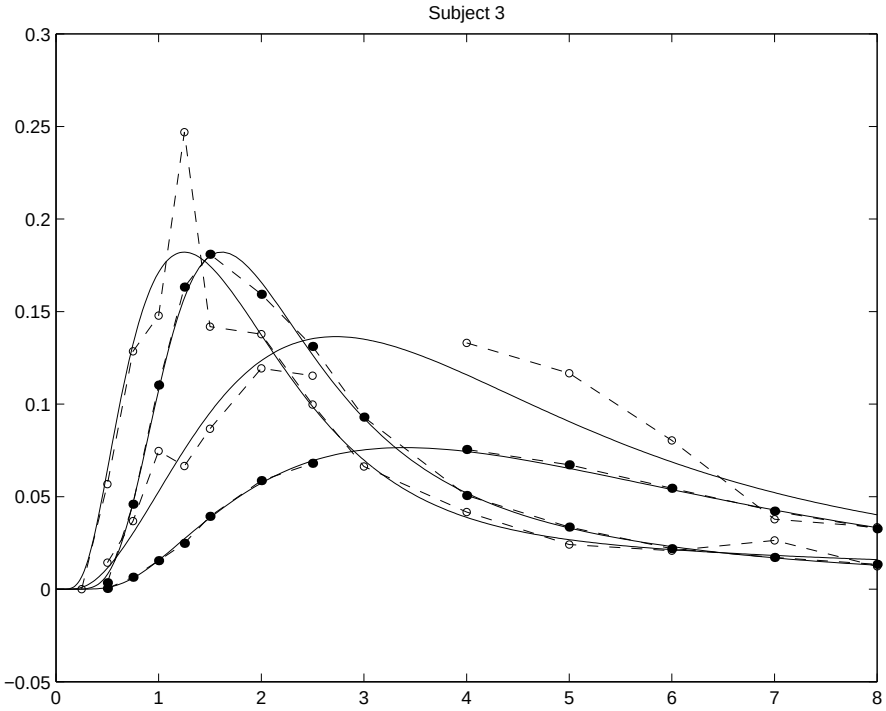

Figure A.3: Subject 3

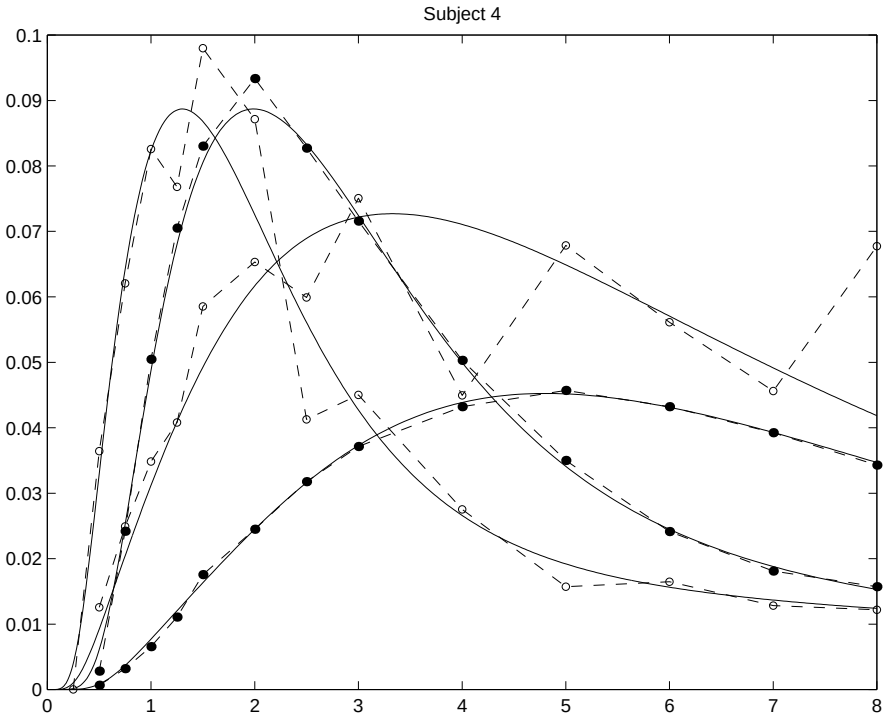

Figure A.4: Subject 4

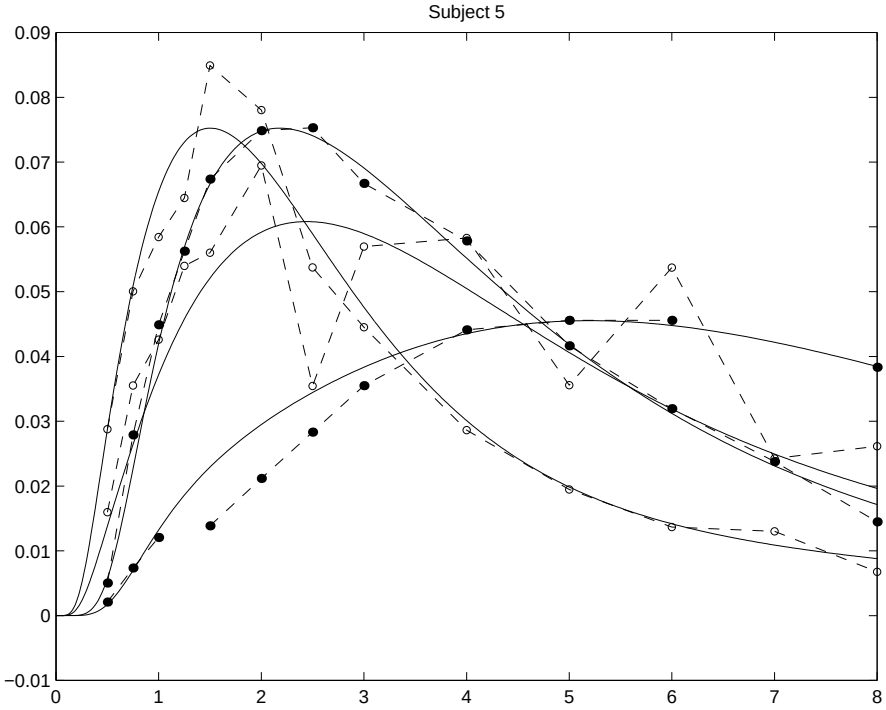

Figure A.5: Subject 5

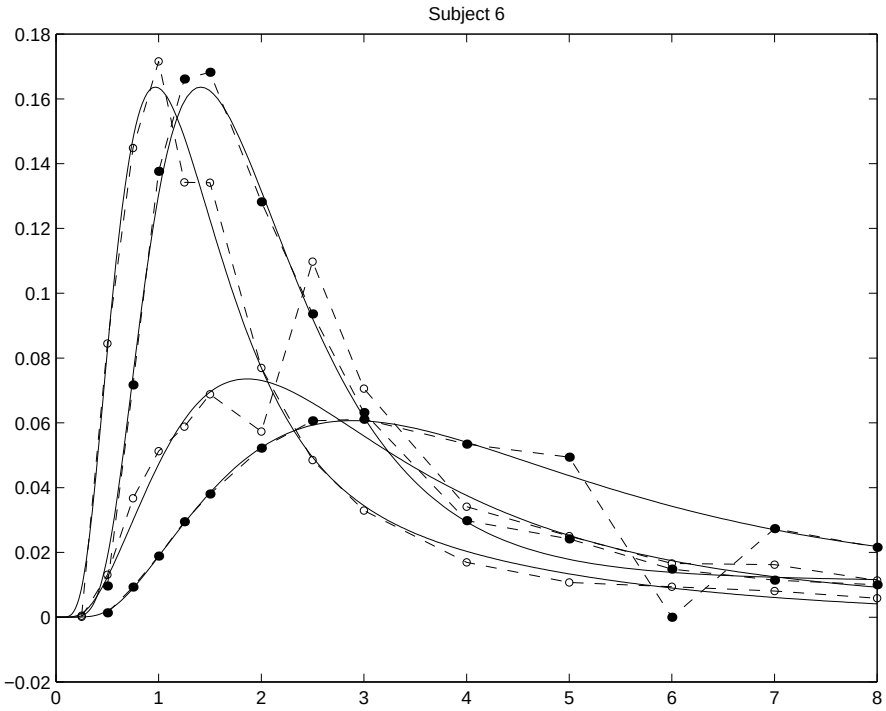

Figure A.6: Subject 6

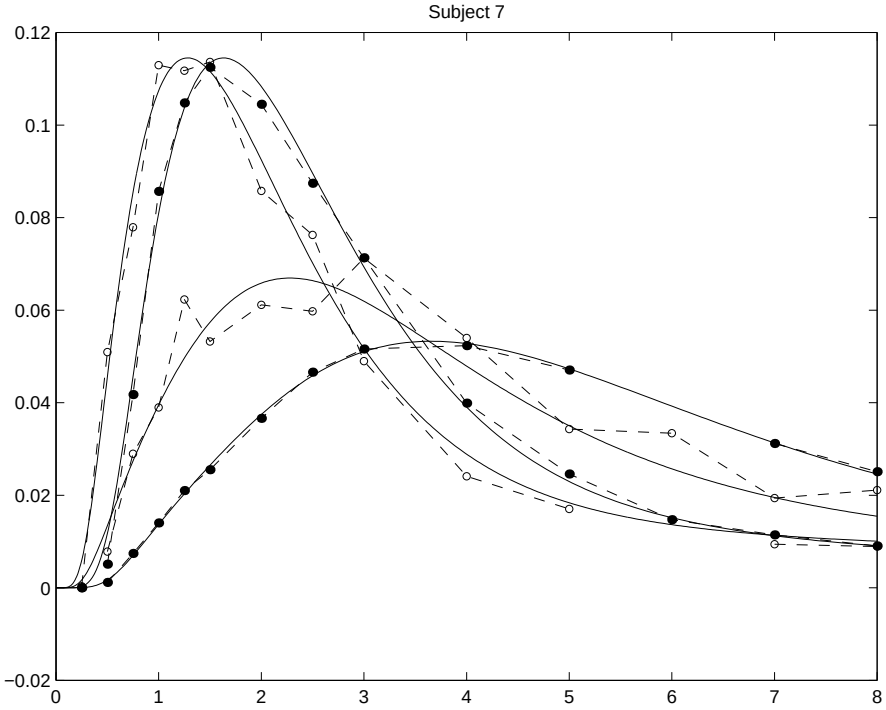

Figure A.7: Subject 7

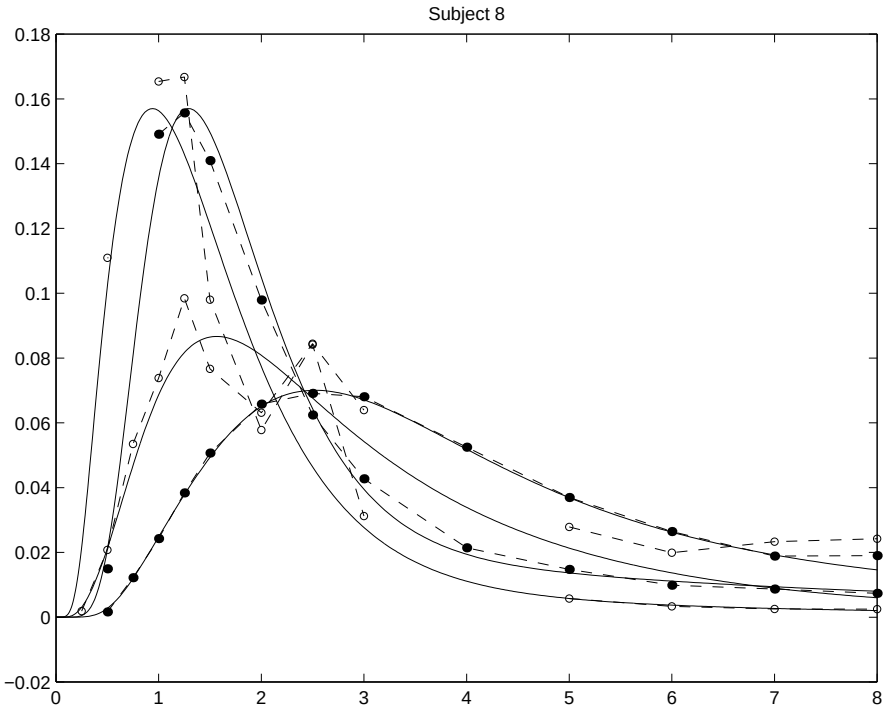

Figure A.8: Subject 8

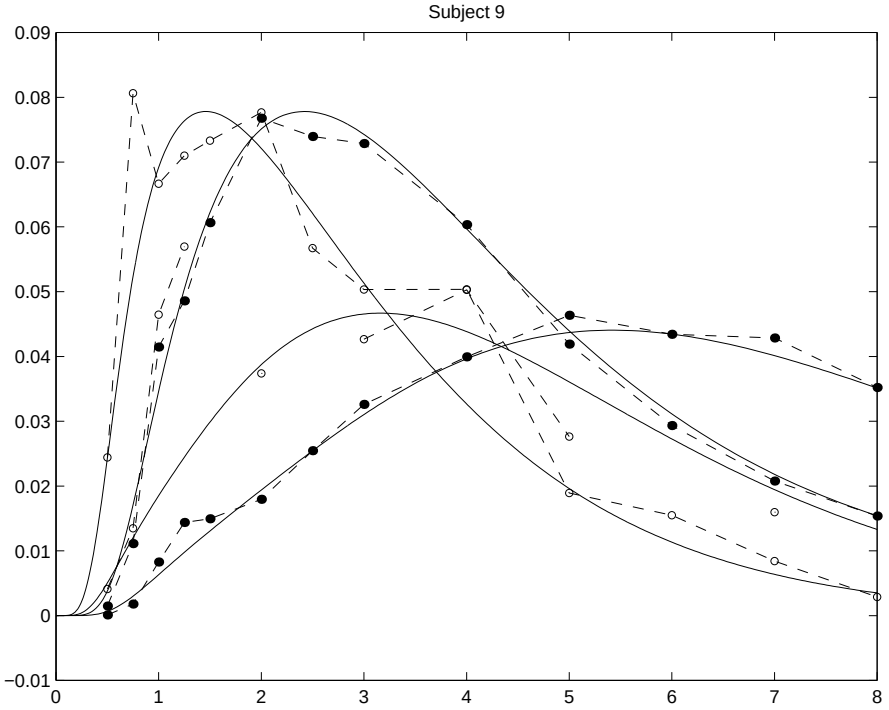

Figure A.9: Subject 9

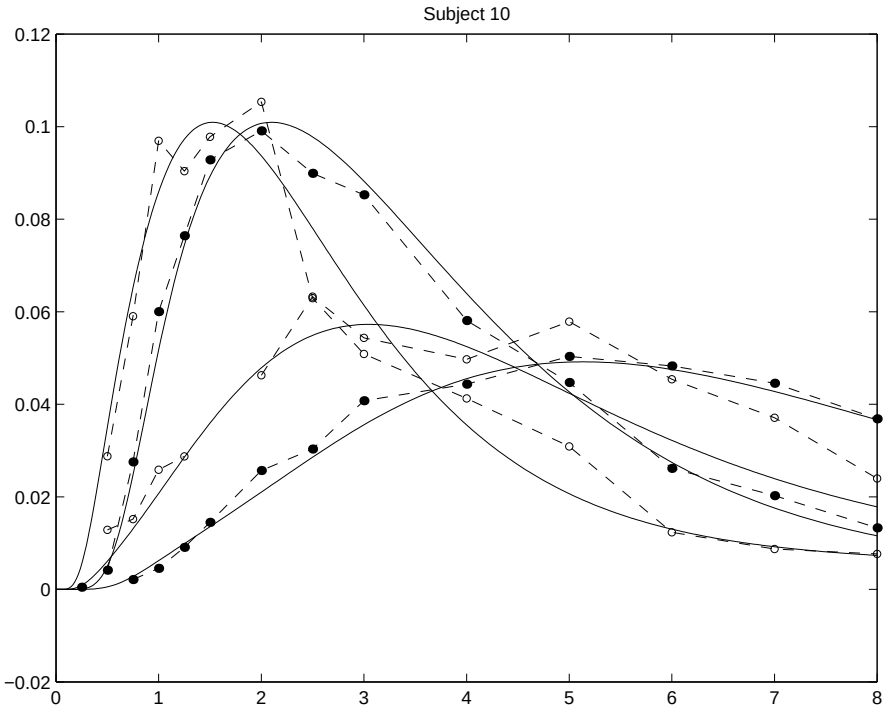

Figure A.10: Subject 10

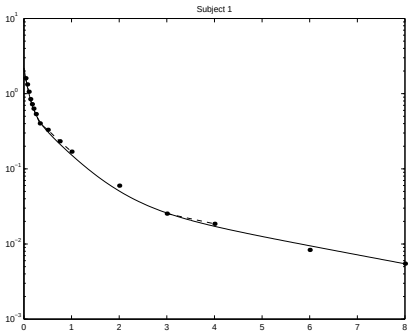

(a) Subject 1

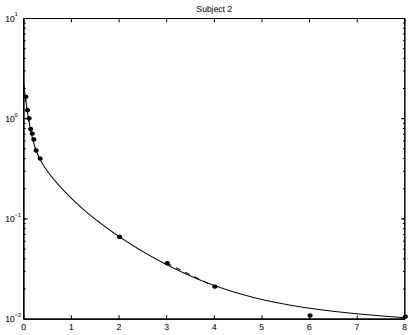

(b) Subject 2

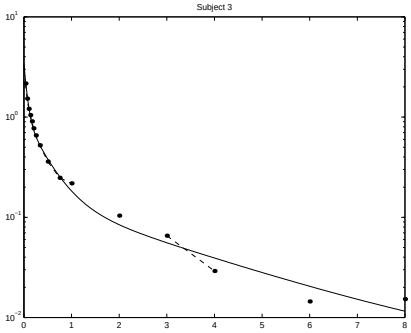

(c) Subject 3

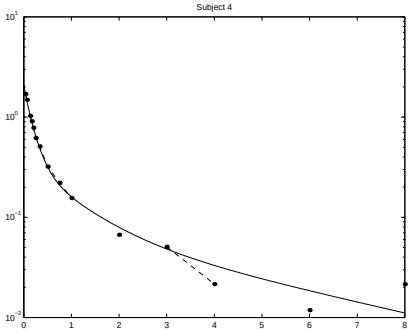

(d) Subject 4

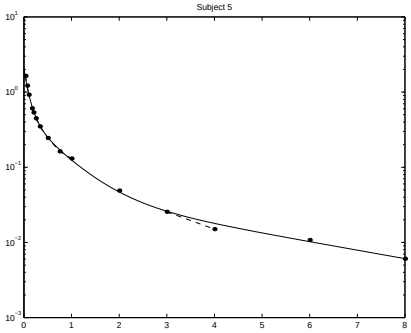

(e) Subject 5

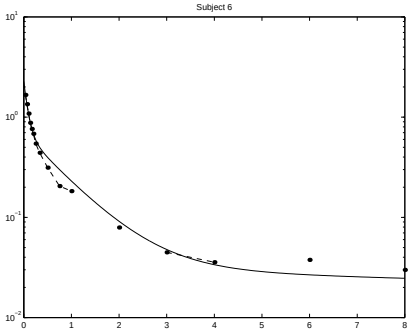

(f) Subject 6

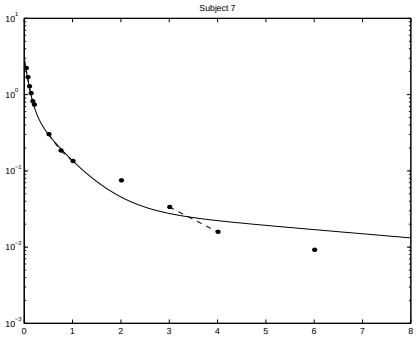

(g) Subject 7

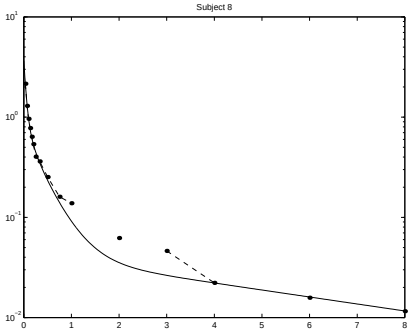

(h) Subject 8

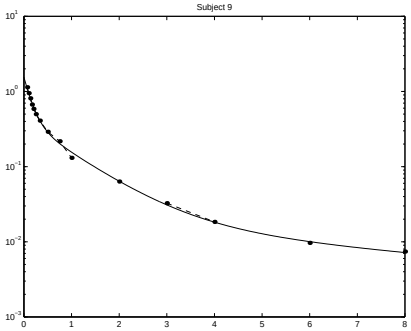

(i) Subject 9

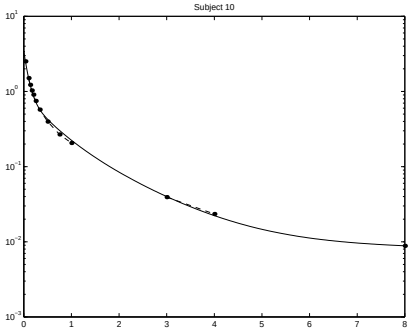

(j) Subject 10

$VLDL_1$ pool sizes

	apoB			TG			TG:apoB		
time	0	4	8	0	4	8	0	4	8
subject									
1	63	56	59	1398	1422	1625	22,3	25,3	27,7
2	47	52	46	1135	1267	1273	24,2	24,3	27,7
3	25	31	36	607	746	826	23,9	24,3	23,3
4	47	43	44	1552	1388	1448	33,2	32,5	32,7
5	155	155	118	3513	3262	3145	22,6	21,0	26,6
6	39	34	29	1152	956	937	29,2	28,1	32,5
7	50	42	26	1242	908	783	24,6	21,7	29,7
8	14	23	25	617	730	740	42,9	31,4	30,1
9	81	82	70	2272	2502	2024	28,1	30,7	28,8
10	90	60	44	2176	1632	1131	24,3	27,1	25,6
mean	61	58	50	1566	1481	1393	28	27	28
stderr	40	38	28	880	817	740	6	4	3

$VLDL_2$ pool sizes

	apoB			TG			TG:apoB		
time	0	4	8	0	4	8	0	4	8
subject									
1	99	91	78	594	520	499	6,0	5,7	6,4
2	66	68	71	381	405	399	5,8	6,0	5,6
3	79	59	59	405	338	360	5,1	5,7	6,1
4	90	121	110	726	893	844	8,1	7,4	7,7
5	116	168	178	930	1104	1104	8,0	6,6	6,2
6	83	87	79	374	407	368	4,5	4,7	4,6
7	89	75	59	489	387	426	5,5	5,2	7,3
8	71	65	85	202	232	211	2,8	3,6	2,5
9	96	112	94	707	649	773	7,4	5,8	8,3
10	154	151	154	694	673	594	4,5	4,4	3,9
mean	94	100	97	550	561	558	6	6	6
stderr	25	38	40	218	271	273	2	1	2

Table A.2: ApoB and TG pool sizes for $VLDL_1$ and $VLDL_2$, [mg]

subject	$k(0,1)$	k$(1,2)$	$k(1,3)$	$k(3,1)$	$k(3,4)$	$k(11,2)$	Inj	p_1	plasma
1	3,24	4,50	5,90	1,21	1,00	0,0093	709	0,59	549
2	2,51	1,49	4,10	5,25	0,10	0,0096	715	0,63	517
3	2,59	6,58	0,42	3,18	0,02	0,0132	622	0,99	183
4	2,46	1,88	8,08	1,89	0,70	0,0066	588	1,00	280
5	3,32	3,35	9,22	2,49	0,59	0,0143	662	0,82	397
6	1,31	4,83	1,24	2,79	0,20	0,0094	729	0,45	718
7	3,61	3,69	3,05	2,44	0,52	0,0100	552	0,49	369
8	5,34	4,88	7,08	7,54	0,40	0,0167	566	0,55	283
9	0,07	2,54	0,03	2,66	0,02	0,0047	764	0,60	829
10	2,44	4,41	0,58	2,45	0,06	0,0114	567	0,44	379
mean	2,69	3,81	3,97	3,19	0,36	0,0105	647	0,65	450
stderr	1,40	1,55	3,43	1,85	0,34	0,0036	78	0,21	203

Table A.3: Plasma parameters for apoB; Inj, injected volume [mg]; p_1, unknown proportion of compartment 1 sampled; plasma, plasmaLeucine [mg].

subject	cat_{10}	$k(0,6)$	$k(0,7)$	$k(0,9)$	$k(6,5)$	$k(7,5)$	$k(9,8)$	$k(10,8)$
1	0,0000	0,8000	0,1931	0,2044	1,1060	0,0477	1,5367	1,1251
2	0,0000	0,0000	0,7688	0,3292	1,0968	2,6947	0,0000	0,4987
3	0,0078	2,3875	0,0059	0,0005	1,3255	0,0068	0,0008	0,5365
4	0,0000	0,9439	0,0144	0,0002	0,9294	0,0319	0,0004	0,3398
5	0,0000	0,5517	0,0003	0,0000	0,4434	0,0000	0,0000	0,3488
6	0,0000	1,3219	2,0000	0,0701	1,4357	1,6288	0,0294	0,6045
7	0,0000	0,0000	0,9290	0,3770	0,9745	0,6800	0,0365	0,5467
8	0,0000	0,0000	4,0000	0,5511	1,9058	0,6454	0,8738	0,6823
9	0,0003	0,0000	0,9670	1,1934	0,5717	0,1583	0,0000	0,5234
10	0,0000	0,0000	2,0000	0,5239	0,7848	0,0000	0,2993	0,2823
mean	0,0008	0,6005	1,0879	0,3250	1,0574	0,5894	0,2777	0,5488
stderr	0,0025	0,7942	1,2733	0,3717	0,4281	0,9036	0,5213	0,2383

Table A.4: Parameters for apoB model.

subject	L_5	L_6	L_7	L_8	L_9	L_10
1	0,51	2,46	0,00	1,50	0,20	0,00
2	1,06	2,43	0,00	0,18	1,12	2,00
3	0,00	3,00	0,00	0,12	0,69	0,17
4	0,00	2,50	0,00	0,08	0,10	0,00
5	0,57	4,00	0,00	0,29	2,00	0,23
6	0,47	0,47	0,00	0,47	0,01	0,47
7	1,50	0,00	1,31	2,12	3,00	0,00
8	0,46	6,00	3,00	2,42	0,00	6,00
9	0,02	2,21	0,00	0,03	1,56	0,62
10	0,00	2,50	0,00	0,15	3,00	0,20
mean	0,46	2,56	0,43	0,74	1,17	0,97
stderr	0,50	1,67	0,99	0,92	1,18	1,87

Table A.5: Parameters for TG model.

subject	$k(14,13)$	$k(14,21)$	$k(21,14)$	$k(22,14)$	plasma
1	0,1583	0,5057	0,5466	1,2442	1151
2	0,2000	1,0642	1,7584	1,6212	712
3	0,1132	0,2466	0,6671	1,1505	498
4	0,0886	0,2259	0,7277	1,4368	654
5	0,2409	0,2603	0,3489	0,6758	1145
6	0,0665	0,6773	1,5188	2,4472	1384
7	0,3160	0,1229	0,5347	0,7068	496
8	0,2000	0,2891	0,1395	1,1567	904
9	0,2000	1,4278	2,9692	3,8188	689
10	0,2027	0,0544	0,5751	0,7541	514
mean	0,1786	0,4874	0,9786	1,5012	815
stderr	0,0746	0,4461	0,8608	0,9697	316

Table A.6: TG liver parameters; plasma, plasmaGlycerol [mg].

	TG:apoB $VLDL_1$		TG:apoB $VLDL_2$		$VLDL_1$: $VLDL_2$	
subject	Prod	Pool	Prod	Pool	Prod	Pool
1	44	25	21	5,9	2,1	4,3
2	37	25	18	5,8	2,0	4,4
3	32	24	10	5,6	3,3	4,2
4	42	33	20	8,0	2,2	4,1
5	66	23	28	6,7	2,4	3,5
6	18	15	7	4,6	2,7	3,3
7	55	24	28	5,9	2,0	4,1
8	59	31	6	3,0	9,5	10,4
9	48	29	14	7,2	3,5	4,1
10	32	20	10	4,2	3,2	4,8
mean	43	25	16	5,7	3,3	4,7
stderr	14	5	8	1,5	2,3	2,0

Table A.7: TG to apoB ratios for $VLDL_1$ and $VLDL_2$. Prod, ratio in newly secreted particles; Pool, ratio in the pools, compare with table A.2.

Appendix B

Calculated values, formulas

The following quantities was calculated for all subjects. (The factor 0.1212 in apoB is the conversion from leucine mass to apoB mass. The factor $882/92$ comes from that the TG have a molecular weight of 882 and glycerol have a molecular weight of 92.)

Fractional Catabolic Rate, FCR The total loss from each fraction in pools/day.

$$\begin{aligned}
\mathbf{FCR}^{\text{apoB}}_{\text{VLDL}_1} &= \frac{\text{FLUX}(0,6)+\text{FLUX}(8,6)+\text{FLUX}(0,7)}{Q_5+Q_6+Q_7},\\
\mathbf{FCR}^{\text{apoB}}_{\text{VLDL}_2} &= \frac{\text{FLUX}(0,10)+\text{FLUX}(0,9)}{Q_8+Q_9+Q_{10}},\\
\mathbf{FCR}^{\text{TG}}_{\text{VLDL}_1} &= \frac{\text{FLUX}(0,15)+\text{FLUX}(0,16)+\text{FLUX}(0,17)+\text{FLUX}(18,16)}{Q_{15}+Q_{16}+Q_{17}},\\
\mathbf{FCR}^{\text{TG}}_{\text{VLDL}_2} &= \frac{\text{FLUX}(0,18)+\text{FLUX}(0,19)+\text{FLUX}(0,20)}{Q_{18}+Q_{19}+Q_{20}}.
\end{aligned}$$

Fractional Direct Catabolic Rate, FDCR The loss due to direct catabolism from each fraction in pools/day. (Same as the $\mathbf{FCR}$ for VLDL_2)

$$\begin{aligned}
\mathbf{FDCR}^{\text{apoB}}_{\text{VLDL}_1} &= \frac{\text{FLUX}(0,6)+\text{FLUX}(0,7)}{Q_5+Q_6+Q_7},\\
\mathbf{FDCR}^{\text{TG}}_{\text{VLDL}_1} &= \frac{\text{FLUX}(0,15)+\text{FLUX}(0,16)+\text{FLUX}(0,17)}{Q_{15}+Q_{16}+Q_{17}}.
\end{aligned}$$

Fractional Transfer Rate, FTR The transfer rate from VLDL_1 to VLDL_2 in pools/day. (Same as $\mathbf{FCR}-\mathbf{FDCR}$)

$$\begin{aligned}
\mathbf{FTR}^{\text{apoB}}_{\text{VLDL}_1} &= \frac{\text{FLUX}(8,6)}{Q_5+Q_6+Q_7},\\
\mathbf{FTR}^{\text{TG}}_{\text{VLDL}_1} &= \frac{\text{FLUX}(18,16)}{Q_{15}+Q_{16}+Q_{17}}.
\end{aligned}$$

Direct production The direct production from the liver.

$$
\begin{aligned}
\mathrm{DirProd}^{\mathrm{apoB}}_{\mathrm{VLDL}_1} &= \mathrm{FLUX}(11,2) F^{\mathrm{apoB}}_{\mathrm{VLDL}_1} 24/0.1212, \\
\mathrm{DirProd}^{\mathrm{apoB}}_{\mathrm{VLDL}_2} &= \mathrm{FLUX}(11,2) F^{\mathrm{apoB}}_{\mathrm{VLDL}_2} 24/0.1212, \\
\mathrm{DirProd}^{\mathrm{TG}}_{\mathrm{VLDL}_1} &= \mathrm{FLUX}(22,14) F^{\mathrm{TG}}_{\mathrm{VLDL}_1} 24 * 882/92, \\
\mathrm{DirProd}^{\mathrm{TG}}_{\mathrm{VLDL}_2} &= \mathrm{FLUX}(22,14) F^{\mathrm{TG}}_{\mathrm{VLDL}_2} 24 * 882/92.
\end{aligned}
$$

Bibliography

[1] D.H. Anderson *Compartmental Modeling and Tracer Kinetics*. Lecture Notes in Biomathematics. Volume 50, Springer. ISBN 3-540-12303-2, (1983).

[2] K.G. Andersson and L-C. Böiers *Ordinära differentialekvationer*. Studentlitteratur, ISBN 91-44-29952-4, (1992).

[3] U.M. Ascher and L.R. Petzold *Computer Methods for Ordinary Differential Equations and Differtial-Algebraic Equations*. SIAM, ISBN 0-89871-412-5, (1998).

[4] Y. Bard *Nonlinear Parameter Estimation* Academic Press, ISBN 0-12-078250-2, (1974).

[5] N.R. Draper and H. Smith *Applied Regression Analysis* Third Edition, Wiley, ISBN 0-471-17082-8, (1998).

[6] B.A. Griffin and C.J. Packard *Metabolism of VLDL and LDL subclass*. Current Opinion in Lipidology. Volume 5, p 200-206. Arterioscler Thromb Vasc Biol. Volume 21, p 1494-1500, (1994).

[7] R.B. Kellogg and A.B. Stephens *Complex Eigenvalues of a Non-Negative Matrix with a Specified Graph*. Linear Algebra and its Applications. Volume 20, p 179-187, (1978).

[8] R. Malmström *Acute regulation of VLDL APO B METABOLISM in healthy subjects and in patients with type 2 diabetes*. PhD thesis, ISBN 952-91-0689-0, (1999).

[9] C. J. Packard et al. *Apolipoprotein B metabolism and the distribution of VLDL and LDL subfractions*. Journal of lipid research. Volume 41, p 305-317, (2000).

[10] C.J. Packard, A. Gaw, T. Demant and J. Shepherd *Development and application of a multicompartmental model to study very low density lipoprotein subfraction metabolism*. Journal of Lipid Research. Volume 36, p 172-187, (1995).

[11] F. Pont, L. Duvillard, B. Vergès and P. Gambert *Development of Compartmental Models in Stable Isotope Experiments Application to Lipid Metabolism*. Arterioscler Thromb Vasc Biol. Volume 17, p 853-860, (1998).

[12] G.A.F. Seber and C.J. Wild *Nonlinear Regression*. Wiley, ISBN 0-471-61760-1, (1989).

[13] K. Tomiyasu et al. *Differential Metabolism of Human VLDL According to Content of ApoE and ApoC-III*. Arterioscler Thromb Vasc Biol. Volume 21, p 1494-1500, (2001).

[14] D.E. Vance and J. Vance (editors)*Biochemistry of Lipids, Lipoproteins and Membranes*. New Comprehencive Biochemistry. Volume 31. ELSEVIER, ISBN 0-444-82364-6, (1996).

[15] D. White and M. Baxter (editors)*Hormones And Metabolic Control*. Second edition, ISBN 0-340-56355-9, (1994).

[16] L.A. Zech, S.M. Grundy, D. Steinberg and M. Berman *Kinetic Model for Production and Metabolism of Very Low Density Lipoprotein Triglycerides.* Journal of Clinical Investigation. Volume 63, p 1262-1273, (1979).

[17] *SAAMII user guide.* SAAM Institute, Inc., Seattle, WA. (1998).